

AD 705989

**R 670**

Technical Report

DISPLACEMENT OF LATERALLY LOADED  
STRUCTURES IN NONLINEARLY  
RESPONSIVE SOIL

April 1970

Sponsored by

NAVAL FACILITIES ENGINEERING COMMAND



NAVAL CIVIL ENGINEERING LABORATORY

Port Hueneme, California

This document has been approved for public  
release and sale; its distribution is unlimited.

63

## DISPLACEMENT OF Laterally LOADED STRUCTURES IN NONLINEARLY RESPONSIVE SOIL

Technical Report R-670

YF 38.534.001.01.002

by

H. L. Gill and K. R. Demars

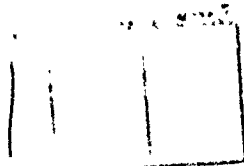
### ABSTRACT

Quantitative information on the response of soil in natural deposits to lateral loadings was obtained by the performance of field tests in conjunction with theoretical studies and in-situ and laboratory determinations. The field tests utilized a segmental pile, a lateral plate loading device, rigid poles subjected to lateral loads, and full-scale laterally loaded piles. Results of the final series of field tests and analytical studies in the program are presented in this report, along with the design recommendations formulated on the basis of the research.

Procedures were developed for the prediction of nonlinear lateral soil pressure-displacement relationships applicable to undisturbed deposits of both cohesive and noncohesive soils using easily measured conventional engineering properties of the soil. These procedures were utilized in the development of design procedures for laterally loaded piles in nonhomogeneous layered soil systems. An iterative solution of the laterally loaded pile problem utilizing a digital computer was developed, and a similar iterative solution for hand computations in a tabular form was evolved for use in cases where a computer cannot be used.

  
This document has been approved for public release and sale; its distribution is unlimited.

Copies available at the Clearinghouse for Federal Scientific & Technical  
Information (CFSTI), Sills Building, 5285 Port Royal Road, Springfield, Va. 22151



## CONTENTS

	page
INTRODUCTION .....	1
Subject and Purpose of Report .....	1
Background .....	1
Experimental Work .....	1
Pile Theory .....	2
Rectangular Hyperbola .....	5
Approach and Scope .....	6
TEST PROGRAM AND PROCEDURES .....	8
Description of Test Site .....	8
Procedures for the Segmental Pile Tests .....	9
Procedures for the Lateral Load Tests on Piles .....	12
TEST RESULTS .....	15
Soil Properties .....	15
Segmental Pile Test Data .....	15
Data from Lateral Load Tests of Piles .....	21
THEORETICAL STUDY .....	21
Initial Slope of Soil Pressure-Displacement Curves .....	24
Lateral Bearing Capacity .....	29
Computation of Lateral Soil Pressure-Displacement Diagrams	31
Cohesive Soil .....	31
Granular Soil .....	31
Repetitive Loadings .....	32
Computed Pile Response .....	33
Computational Procedure .....	33
Computer Solutions .....	33

	page
TABULAR SOLUTION FOR LATERALLY LOADED PILES . . . .	35
Example Problem . . . . .	39
CONCLUSIONS . . . . .	49
ACKNOWLEDGMENTS . . . . .	50
APPENDIX—COMPUTER PROGRAM . . . . .	51
REFERENCES . . . . .	56
LIST OF SYMBOLS . . . . .	59

This Document Contains  
Missing Page/s That Are  
Unavailable In The  
Original Document

OR are  
Blank pgs.  
that have  
Been Removed

**BEST  
AVAILABLE COPY**

## INTRODUCTION

### Subject and Purpose of Report

Presented in this report are the results of a study conducted at the Naval Civil Engineering Laboratory (NCEL) to develop realistic criteria for the design and analysis of laterally loaded, pile-supported foundations. The overall objective of the program was to develop procedures for determining soil moduli and variations of soil moduli with depth, width of loaded area, magnitude of displacement, and repetition of loading. For expediency, the study was directed toward a consideration of the laterally loaded pile problem, in order that the relatively large body of theoretical and experimental information on that subject could be exploited. Results of segmental pile tests, lateral load tests on full-scale piles, and tests to determine in-situ soil properties were used to fulfill the objectives of the study. Details of these tests and the associated results are outlined.

Of particular interest in the study of laterally loaded piles was the development of a design method capable of accounting for the nonlinear soil pressure-displacement characteristics (p-y curves) of naturally occurring heterogeneous soil deposits. The procedures which were evolved to relate the load-displacement characteristics of soil-pile systems utilize a closed-form expression comprised of parameters quantifying the field boundary conditions. The resulting expression takes the form of a relatively simple rectangular hyperbola, and a major portion of the research effort has been devoted to a correlation of the terms in the hyperbola to measurable physical properties of the pile and the soil deposit. Results of the studies are presented in the form of a digital computer solution or, as an alternate, a less exact but more expedient slide rule-type of solution in tabular form.

### Background

**Experimental Work.** Test programs of several types have been performed at NCEL in order to provide quantitative information on the p-y curves of soil. Rigid pile tests,<sup>1</sup> lateral plate loading tests,<sup>1,2,3</sup> lateral load tests on full-scale piles,<sup>4</sup> and segmental pile tests<sup>4, 5</sup> have been performed in

deposits of granular and cohesive soils. The data obtained have indicated the form of the resulting p-y curves, and they have given a tentative indication of procedures for computing the necessary boundary conditions for the pile solutions. Subsequent to the time that these tests were performed, additional segmental pile tests and lateral load tests on full-scale piles were performed in a soil deposit at El Centro, California, in order to provide further background for the prediction of p-y curves. Data from these later tests are presented in this report.

**Pile Theory.** The basic differential equation for a vertically embedded pile subjected to a lateral load and/or a bending moment is

$$EI \frac{d^4 y}{dz^4} = -pB \quad (1)$$

where EI is the flexural stiffness of the pile, y is the horizontal displacement of a differential longitudinal segment of the pile located at a depth Z below the ground surface, the term p represents the corresponding average horizontal soil pressure on the pile at that depth, and B denotes the width of the pile. Equation 1 is applicable for cases where the axial load on the pile is less than about 10% of the buckling load;<sup>6</sup> for greater axial loads, a second-order differential term is required. The quantity pB/y is usually referred to as the modulus of horizontal subgrade reaction, k.

The complexity of Equation 1 has forced analysts to make simplifying assumptions regarding the interrelationships between the various parameters affecting pile response, and although some of the assumptions have been proven conclusively to be in error, their use has been continued because of a lack of a suitable substitute. For example, the nonlinear p-y curves have been represented by a linear relationship as indicated by the dash line in Figure 1. Use of this assumption can result in quite conservative results for small displacements or possibly unconservative results for displacements greater than  $y_1$ . At any rate, it is evident that the factor of safety in the analysis would vary considerably with the magnitude of the displacement. This variation is especially prominent in the top few feet of soil where the greatest pile displacements occur and where the most resistance to horizontal displacement is manifested.<sup>7</sup> The resulting error could be significant for sea floor foundations or for other installations in sediments of low consistency where relatively large displacements might occur.

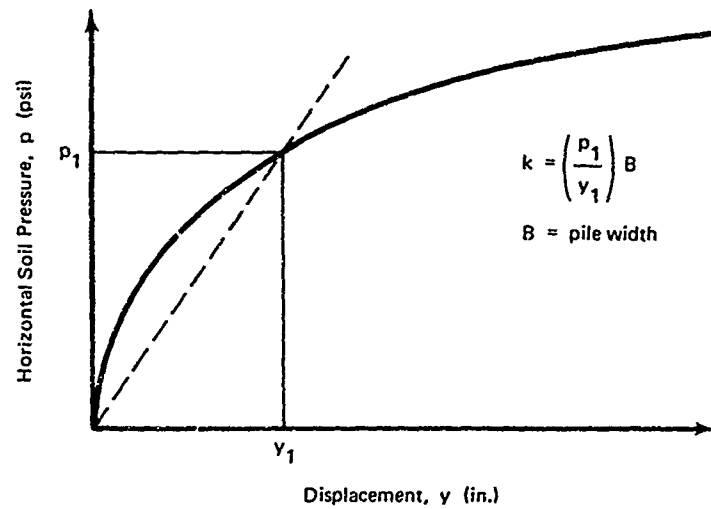


Figure 1. Typical horizontal soil pressure-displacement diagram for a pile element.

Another simplifying assumption which has been used generally is associated with the variation in the assumed values of  $k$  with depth in the soil deposit. Solutions to the problem of laterally loaded piles have been obtained with the variation of  $k$  with depth being assumed to be constant,<sup>7</sup> directly proportional,<sup>8</sup> a step-function,<sup>7</sup> a hyperbolic function,<sup>9</sup> or an exponential function.<sup>10</sup> These assumed relationships of  $k$  with depth are illustrated in Figure 2. It is clear, however, that the deficiencies associated with these assumptions are a result not only of the typical nonhomogeneity of naturally occurring soil deposits, but also as a result of variations in the magnitudes of horizontal displacement along the length of the pile and nonlinear  $p$ - $y$  curves. A more rigorous approach to the problem is necessary in order to incorporate the nonlinear soil pressure-deformation-depth characteristics of naturally occurring soil deposits.

Recent advancements in computer technology have removed most of the restrictions on mathematically solvable variations of soil pressure with depth and displacement. Analog computers have been used to study the behavior of laterally loaded piles,<sup>7</sup> and digital computers have supplied a solution to Equation 1 by means of a difference-equation method and an



iterative process capable of adjusting a linear soil parameter until soil-pile compatibility was obtained.<sup>8</sup> Either type of computer is capable of providing a solution which incorporates nonlinear soil characteristics and varying pile geometry for which Equation 1 becomes

$$f(Z) \frac{d^4 y}{dZ^4} = -f(y, Z) \quad (2)$$

where the flexural stiffness of the pile and the nonlinear soil pressure-displacement characteristics are both functions of depth. With the aid of a digital computer, it was possible during this study to consider all parameters influencing lateral soil pressure-displacement relationships without making any attempt to minimize or camouflage the effects of nonlinearity.

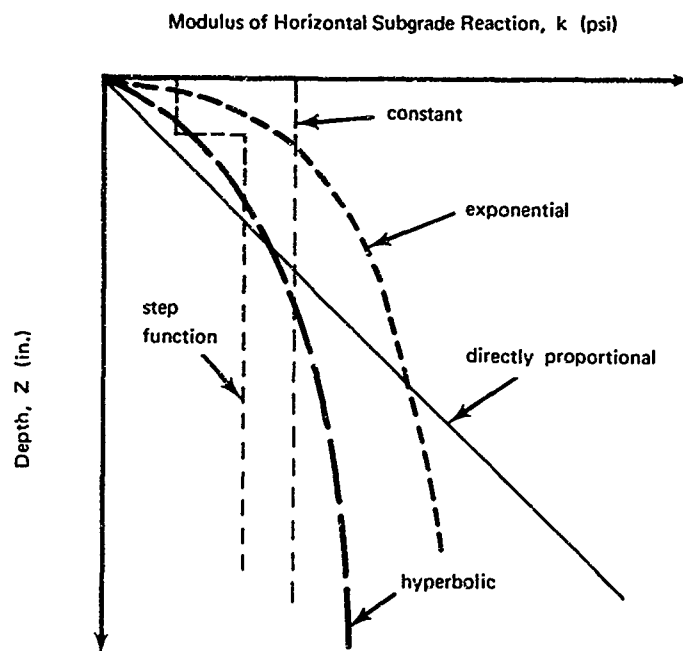


Figure 2. Assumed variations of  $k$  with depth.

A graphical representation of the general problem is presented in Figure 3 for a typical flexible pile subjected to a groundline shear,  $Q_g$ , and a groundline moment,  $M_g$ . Under these loading conditions, the pile would deflect approximately as shown in Figure 3(b). At various locations along the length of the pile, the p-y curves might be similar to those illustrated in Figure 3(c) where the displacement corresponding to each location is denoted by a cross. It is apparent that any distribution of  $k$  with depth could result, and it is equally evident that the resulting magnitudes of  $k$  will change when the pile loading is altered. Thus, the problem becomes one of predicting the p-y curves for a given soil-pile system.

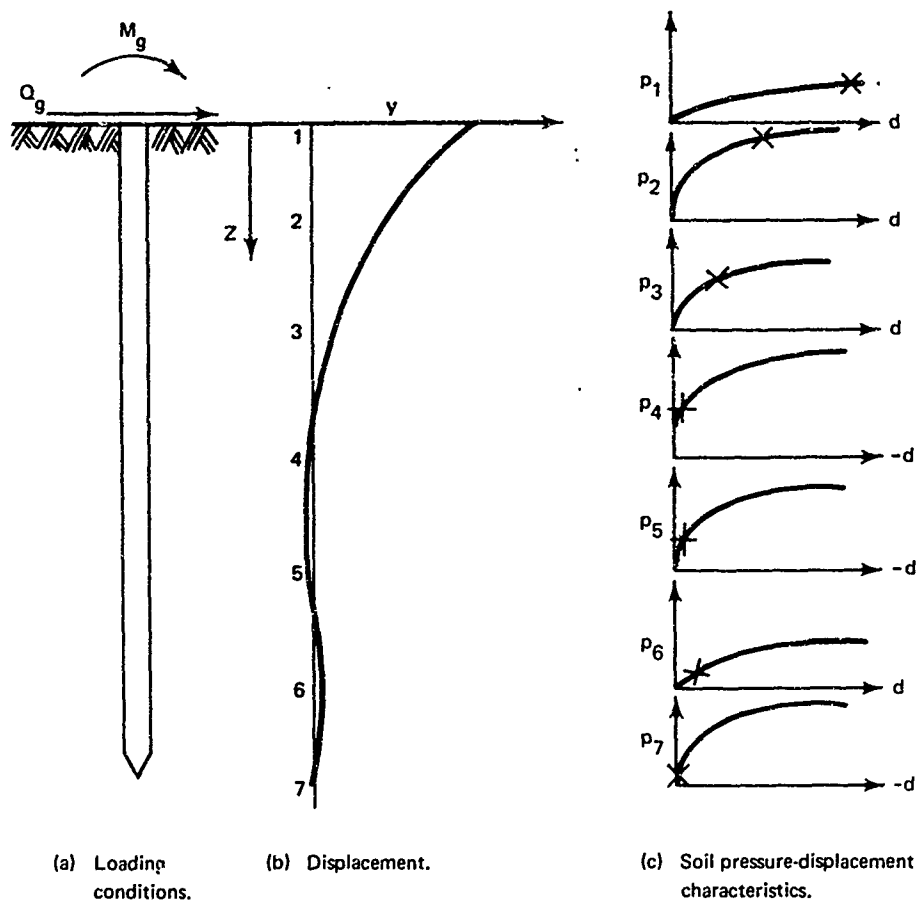


Figure 3. Graphical representation of the problem.

**Rectangular Hyperbola.** A technique for describing a soil's stress-strain (or pressure-deformation) relationship has been proposed. This method, which is based on the characteristics of a rectangular hyperbola,<sup>11</sup>

was found to provide an adequate simulation of the stress-strain relations examined. Also, certain of the hyperbolic parameters were found to be related to the physical characteristics of the soil. These parameters simply describe a soil's nonlinear stress-strain relationship in linear form as described below.

Consider a set of coordinate axes  $p'$  and  $y'$  with a hyperbola as drawn in Figure 4, with the axes as asymptotes. If the  $p'$  axis were translated to the right to the position of the  $p$  axis and if the  $y'$  axis were translated downward to the position of the  $y$  axis, then the hyperbola would resemble the nonlinear soil pressure-displacement curve shown in Figure 1. This hyperbola has two properties that easily permit it to be expressed by an equation in the linear form shown in Figure 5. (Note that the ordinate of Figure 5 is the abscissa divided by the ordinate of Figure 4.) These two properties are: (1) the inverse of the slope of a tangent to the hyperbola at the translated origin,  $B/k_i$ , (Figure 4), represents the intercept of the straight line on the vertical axis of Figure 5; and (2) the inverse of the ultimate value of the hyperbola in Figure 4,  $1/p_f$ , approximately represents the slope of the straight line resulting in Figure 5. Therefore, the equation of the rectangular hyperbola is

$$\frac{y}{pB} = \frac{1}{k} = \frac{1}{k_i} + \frac{1}{p_f} \left( \frac{y}{B} \right) \quad (3)$$

Thus, the nonlinear  $p$ - $y$  curves can be represented by the linear equation of the rectangular hyperbola if the magnitudes of the parameters  $k_i$  and  $p_f$  are known. Procedures for predicting these parameters from measurable soil properties and pile characteristics are presented later.

#### Approach and Scope

Field tests with the NCEL 12-inch-diameter segmental pile have been performed in conjunction with lateral load tests on full-scale flexible piles in deposits of cohesive and noncohesive soils. Steel pipe piles with diameters of approximately 4, 8, 12, and 16 inches were used. The results of the segmental pile tests have been used as a guide in the formulation of procedures for predicting the parameters in Equation 3. Results of the lateral load tests on piles have provided further information on these parameters as well as a means for checking the applicability of the theoretical work. In addition, published data from lateral load tests on piles have been utilized to the extent possible in the evaluation of the proposed design procedures.

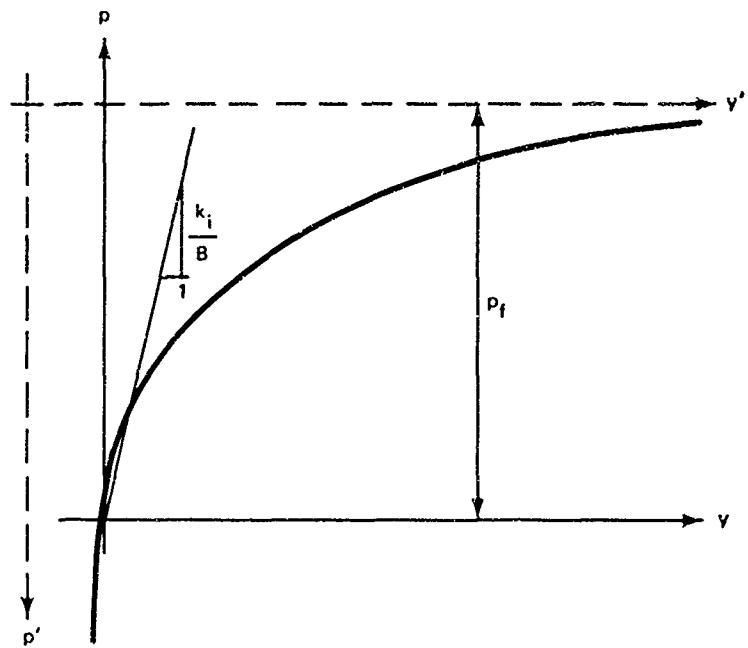


Figure 4. Transposed coordinate axis with typical hyperbola.

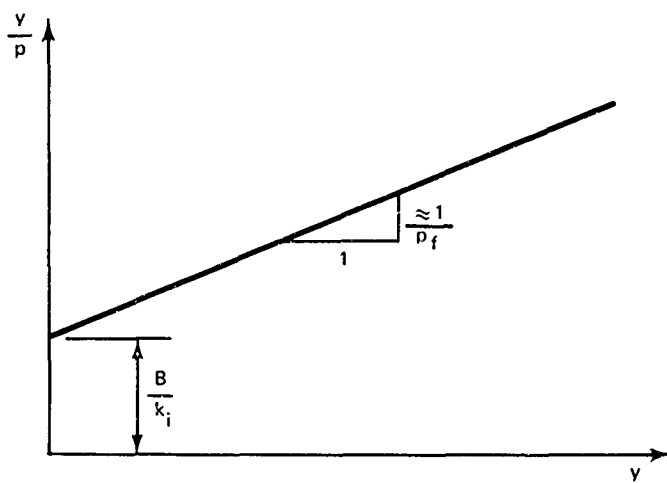


Figure 5. The rectangular hyperbola, a linear form of the hyperbola.

Results of field tests in a granular hydraulic fill and in a deposit of bay mud with a desiccated crust were reported earlier<sup>4</sup> however, significant information from those earlier tests are referred to in this report. Results of a later series of tests in a deposit of cohesive soil near El Centro, California, are presented also in this report. Data from the segmental pile tests, the lateral load tests on piles, and the in-situ and laboratory tests for the determination of soil properties at the El Centro site have been used in conjunction with previously reported test results in order to select realistic criteria for the design of laterally loaded piles. These criteria are outlined for use in conjunction with a digital computer program as listed in Appendix B. In addition, a simplified design method in tabular form is proposed for use when a computer is not available. This simplified procedure can be effected with only a slide rule and existing design charts; however, the same design criteria, with nonlinear p-y curves, is applicable in the simplified approach as well as the computer solution. An example problem is solved in order to provide an illustration of the proposed design procedures.

## TEST PROGRAM AND PROCEDURES

### Description of Test Site

Field tests (the final series in the program) were performed at El Centro Naval Air Station, El Centro, California. That site was chosen because it provided a conveniently accessible deposit of silty clay with a desiccated zone near the surface. Tests were performed at four prepared site locations consisting of two locations with the soil at its natural moisture content (dry locations) and the other two locations with water standing at the surface (flooded locations). The flooding was intended to reduce the effect of large negative pore pressures in the desiccated zone, thereby providing two contrasting soil conditions for the investigation. Flooding was accomplished by constructing a small embankment around the area to be tested and maintaining water to a depth of 1 inch for several days before testing. No tests were conducted until vane shear strength values stabilized in the flooded soil. One of the flooded locations was prepared for the segmental pile tests and the other was prepared for the lateral load tests on piles.

At each location, field vane shear measurements were obtained with a 5-inch-long by 2½-inch-diameter vane which was hand-driven into the soil with a sledge hammer and turned by hand with a torque wrench. A maximum torque was developed at approximately 5 seconds, and the

maximum torque value was recorded for each incremental depth. Torque corrections were made for the soil friction on the vane rod for each vane shear value measured. The resulting values are presented in a later section of the report.

Soil specimens from the upper 10 feet of soil at each location were obtained with 3-inch-diameter, thin-walled sampling tubes using a floating-piston sampler. The samples were returned to the laboratory where classification tests and consolidated-undrained triaxial shear tests were performed. Pertinent results of these tests also are presented in a later section of this report, along with the soil descriptions.

#### **Procedures for the Segmental Pile Tests**

The segmental pile was developed to provide a means for studying the lateral load-supporting characteristics of naturally occurring, undisturbed deposits of soil. This device consists of 12-inch-OD steel tubing installed in a soil deposit in three separate longitudinal segments with all soil excavated from the interior of the segments. The middle or test segment can vary in height and, during the El Centro tests, segment heights of 8 and 12 inches were used. A test is performed by forcing the middle segment horizontally while corresponding loads and displacements are recorded. A cross section of the segmental pile prepared for installation with a 4-inch test segment is presented in Figure 6a. In Figure 6b, the device is shown after driving has been accomplished. In that sketch, the mandrel with its encased specimen of soil has been removed, leaving the segmental pile with a vacated interior to allow the insertion of the loading mechanism. Testing at a greater depth can be accomplished by driving the segmental pile deeper, after realignment of the segments, removal of the loading mechanism, and reinsertion of the mandrel. A retrieval system was developed to recover the two lower segments.

With the mandrel in place, each pile was driven into the soil by a drop-weight type pile driver to a depth such that the center of the test segment was located at least 30 inches below the ground surface. At this point, the mandrel and the interior soil were removed and the loading mechanism was inserted. At the beginning of each test, small pressure increments of 1 psi or less were applied to the test segment in order to define the initial portion of the soil pressure-displacement curves; larger increments were used throughout the remainder of the tests. Each pressure level was maintained constant while displacement-time measurements were recorded. The load level was changed when the segment displacement became negligible during a 5-minute interval. Only the final soil pressure-displacement relationship was considered in the analysis of the data.

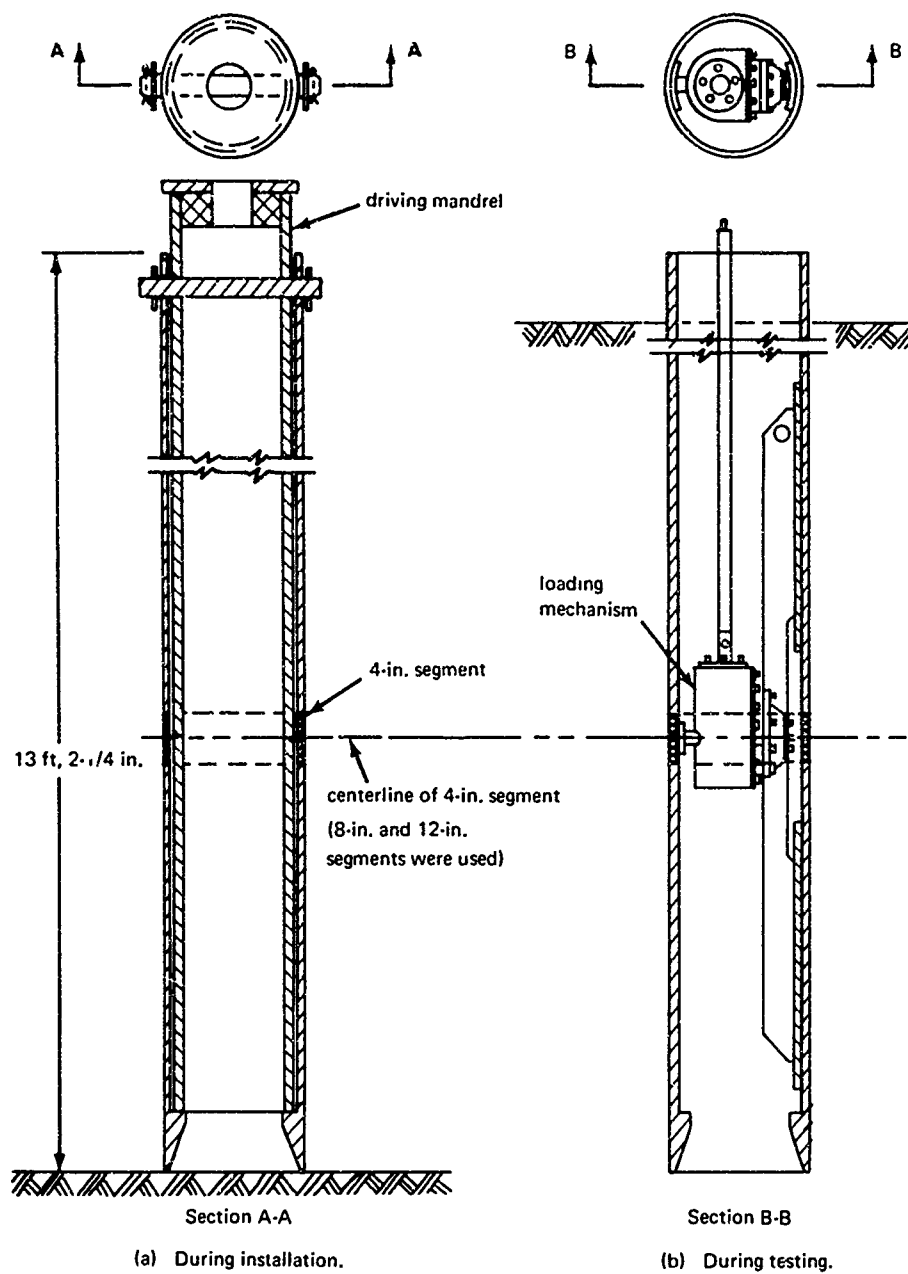


Figure 6. Segmental pile and loading mechanism.

The magnitude of lateral displacement was limited to 0.5 inch or the 15,000-pound load capacity of the loading mechanism. On reaching the capacity of the loading mechanism, the pressure on the test segment was removed in 4 or 5 approximately equal increments. The maximum previous pressure was then reapplied and removed as many as 20 times if displacement limitations permitted. Displacement readings were taken at only the maximum load and after removal of the load during these repetitions. Subsequently, the segment was realigned, the loading mechanism was removed, the mandrel was inserted, and the pile was driven to another test depth.

The program for the segmental pile tests at El Centro is provided in Table 1. After the first three tests in the dry area (D1 through D3) had been performed, it was learned that misalignment of the loading mechanism had created a binding of the loading mechanism with the upper segment, resulting in unreliable measurements during those tests. The remainder of the segmental pile test data were of acceptable quality, and these data are discussed later.

Table 1. Test Program for the Segmental Pile in El Centro Soil

Test No.	Height of Test Segment (in.)	Depth (in.)
Flooded Area		
F1	8	30
F2	8	60
F3	8	108
F4	8	36
F5	12	48
F6	12	78
F7	12	108
Dry Area		
D4	12	30
D5	12	60
D6	12	90
D7	12	114
D8	8	36
D9	8	72
D10	8	110
D11	8	36
D12	12	42



## Procedures for the Lateral Load Tests on Piles

Lateral load tests on flexible piles were conducted to provide information on pile response for use in a theoretical study. A range of pile sizes was considered in order to enable an evaluation of scaling effects. Open-ended, steel, pipe piles of four different sizes ranging from 4.5 to 16 inches in diameter were driven to depths such that a free-standing portion of approximately 3 feet remained for each pile. The piles were designed to have embedded lengths greater than  $4R$  where  $R$  is a relative stiffness factor defined as

$$R = \left( \frac{EI}{k_o} \right)^{0.25} \quad (4)$$

The quantity  $k_o$  is a value of the modulus of horizontal subgrade reaction for a case where the modulus is assumed to be constant with depth. It has been shown analytically that piles with embedded lengths greater than about  $4R$  respond to lateral loadings approximately as if they were embedded to an infinite depth.<sup>7</sup> The impropriety of assuming that  $k$  can be expressed as a simple function of depth without considering magnitudes of displacement and other boundary conditions has been discussed previously, but the use of the assumption for computing necessary pile lengths is an acceptable procedure if conservatively low values of  $k_o$  are assumed. A photograph of the piles embedded at a flooded location is presented in Figure 7.

During the tests, lateral loads were applied to each pile at a point approximately 32 inches above the ground surface in order to provide both a shearing force and a bending moment in the pile at the groundline. A typical test setup is shown in Figure 8 where the cable and hydraulic ram used for applying the loads can be observed. Also shown (less distinctly) in Figure 8 are the four dial indicators, spaced approximately evenly up to 30 inches above the ground surface, for measurements of displacement and slope, and the Dillon dynamometer used to obtain load measurements.

The program for the lateral load tests on piles is given in Table 2 where the test numbers, pile diameters, pile stiffnesses, and depths of embedment are presented. Each lateral load test was conducted in a manner similar to the segmental pile tests. The lateral loads were applied incrementally up to a maximum of 20 kips (the capacity of the loading system)

or until the range of the two top dial indicators was exceeded (about 1.5 inches of displacement at the groundline). Each load was again maintained constant until progressive displacement during a 5-minute interval became negligible.

Table 2. Program for Lateral Load Tests on Piles in El Centro Soil

Test No.	Pile Diameter (in.)	Pile Stiffness (lb-in. <sup>2</sup> )	Depth of Embedment (in.)
Flooded Area			
P1	4.50	$2.26 \times 10^8$	144
P2	8.625	$1.73 \times 10^9$	204
P3	12.75	$8.38 \times 10^9$	264
P4	16.00	$1.686 \times 10^{10}$	324
Dry Area			
P5	4.50	$2.26 \times 10^8$	144
P6	8.625	$1.73 \times 10^9$	204
P7	12.75	$8.38 \times 10^9$	264
P8	16.00	$1.686 \times 10^{10}$	324



Figure 7. Piles embedded in flooded location.



Figure 8. Lateral load test in progress.

## TEST RESULTS

Data obtained from the soil property determinations, the segmental pile tests, and the lateral load tests on piles is presented and discussed. An analysis of the test data is included in a later section of the report.

### Soil Properties

The soil at the El Centro site consists of a brown, silty clay and clayey silt with an occasional trace of fine sand. It is classified as ML to CL by the unified soil classification system. A desiccated crust approximately 60 inches in depth exists at the site, and the water table was located at a depth of approximately 144 inches.

Index properties of the soil are exhibited in Figure 9, and the field vane shear strength test results are plotted in Figure 10. Values plotted represent averaged values for several tests at each location, and the test data for the shallow depths of interest typically fell within plus or minus 30% of the values plotted. It is noted that the effect of flooding apparently becomes negligible at depths below 50 inches. In the zone from 120 to 160 inches depth, the fairly large difference in the values obtained for the two areas is believed to be a result of the lack of resolution of the measurements, brought about by the relatively large corrections for rod friction which were necessary at the greater depths. The discrepancy is of no consequence because the behavior of the laterally loaded piles is controlled almost entirely by the characteristics of the soil at shallower depths.

The effect of desiccation on the vane shear strengths is readily apparent in Figure 10. It can be seen that the reductions in negative pore pressures in the desiccated crust as a result of flooding led to appreciably lower shear strengths in the flooded zone. Therefore, considerably greater pile displacements for corresponding magnitudes of loading were expected for the flooded location in comparison with the dry location.

### Segmental Pile Test Data

When soil pressure was plotted versus corresponding magnitudes of displacement, most of the data resulted in S-shaped curves, i.e., a disproportionately large amount of displacement occurred at low pressure levels. The data points from one typical test are presented in Figure 11. The reversed curvature resulted from alignment difficulties encountered with the loading mechanism at the start of the tests. Consequently, a method for locating the correct zero displacement was needed, and two methods were employed.

The first method involved simply correcting the initial portion of the curve by eye. A second method involved the plotting of soil pressures on an arithmetic scale versus corresponding magnitudes of displacement on a logarithmic scale. The upper portion of the S-shaped curves, which were assumed to be the most valid portion, plotted as a straight line; so by extending this straight line to the logarithmic axis, it was possible to locate an apparent point for zero displacement. Both methods produced similar results and an average was used when a discrepancy occurred.

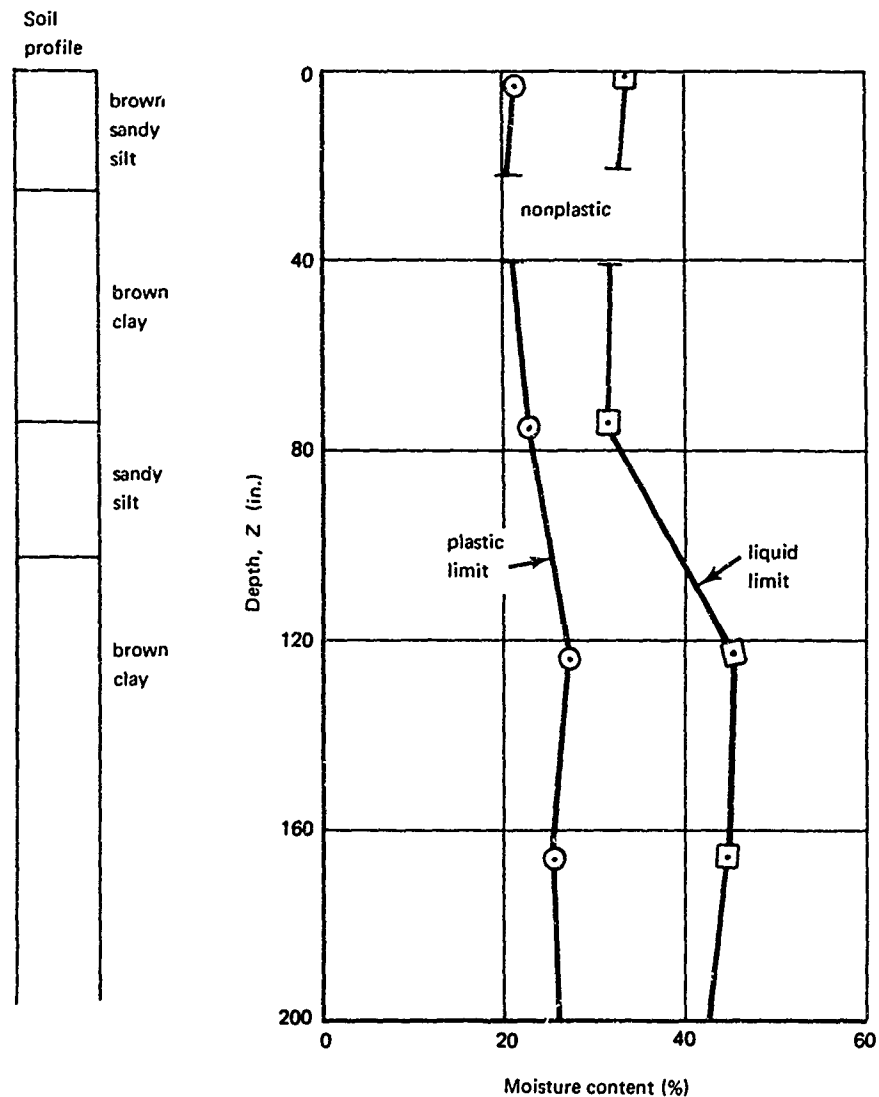


Figure 9. Index properties of El Centro soil.

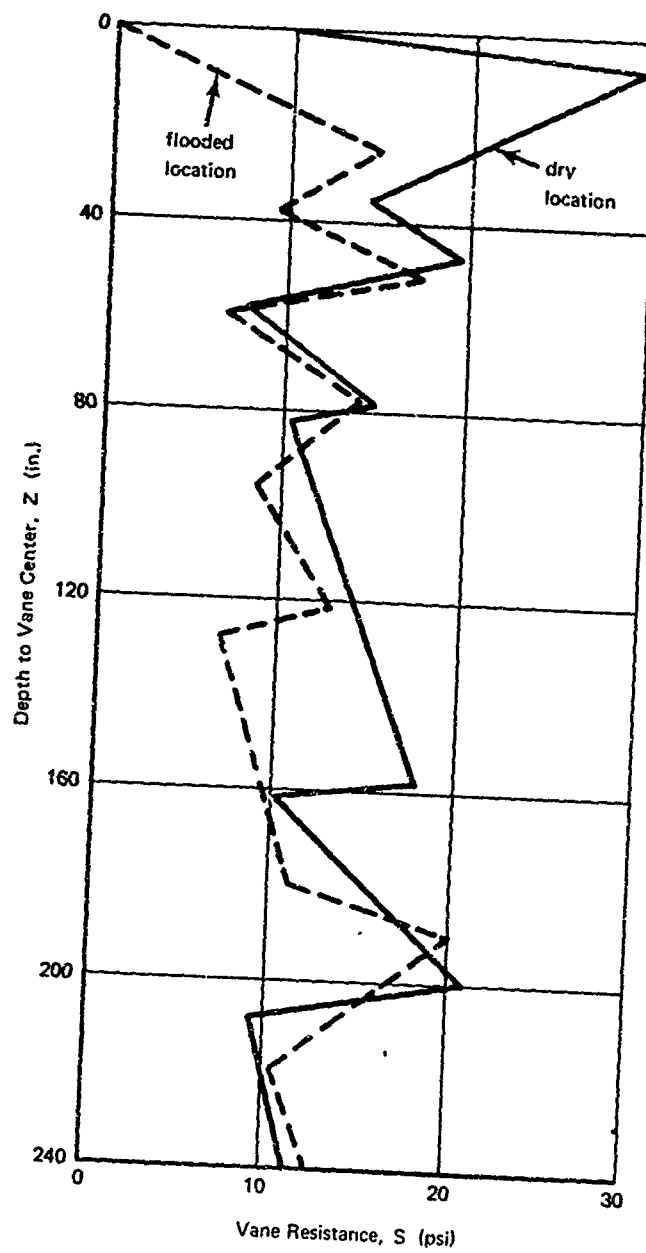


Figure 10. Average vane resistance versus depth in the El Centro soil.

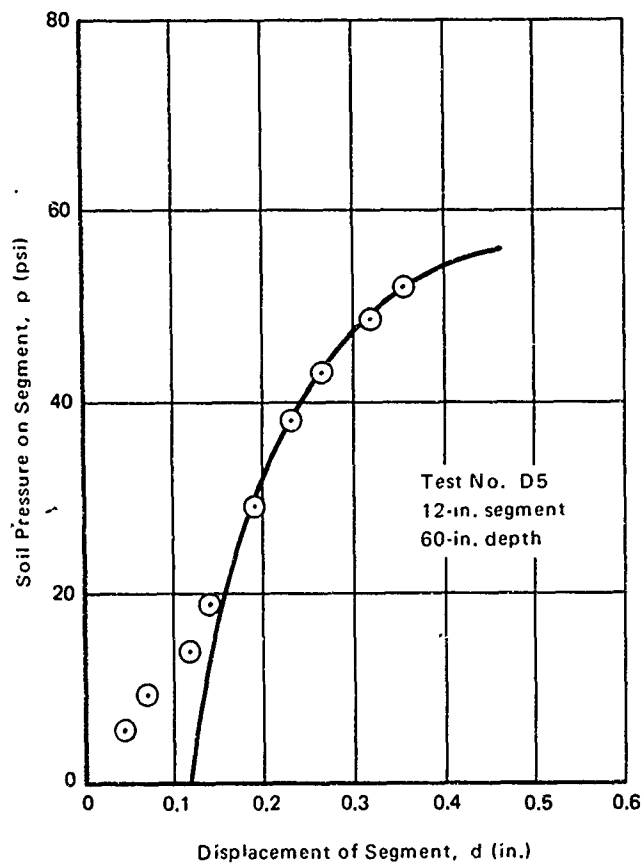


Figure 11. Typical S-shaped soil pressure-displacement curve from segmental pile tests with correction.

Figure 12 contains the corrected data obtained from segmental pile tests. The data from the first loading during each test are presented in the form of soil pressure-displacement curves grouped according to segment size and test location. Each curve is characteristically concave-downward and similar to the modified hyperbola presented in Figure 3.

Data from subsequent cycles of the maximum load during the tests are presented in Figure 13 where displacement, expressed as a percentage increase over the peak displacement occurring during the first loading cycle, is plotted as a function of the number of load applications. An extrapolation of some of the test data to an infinite number of repetitions indicates that more than a 100% increase in displacement as a result of repetitive lateral loading in the El Centro soil can be expected in some cases. However, during a majority of the tests it appeared that the increase would not have exceeded 50%.

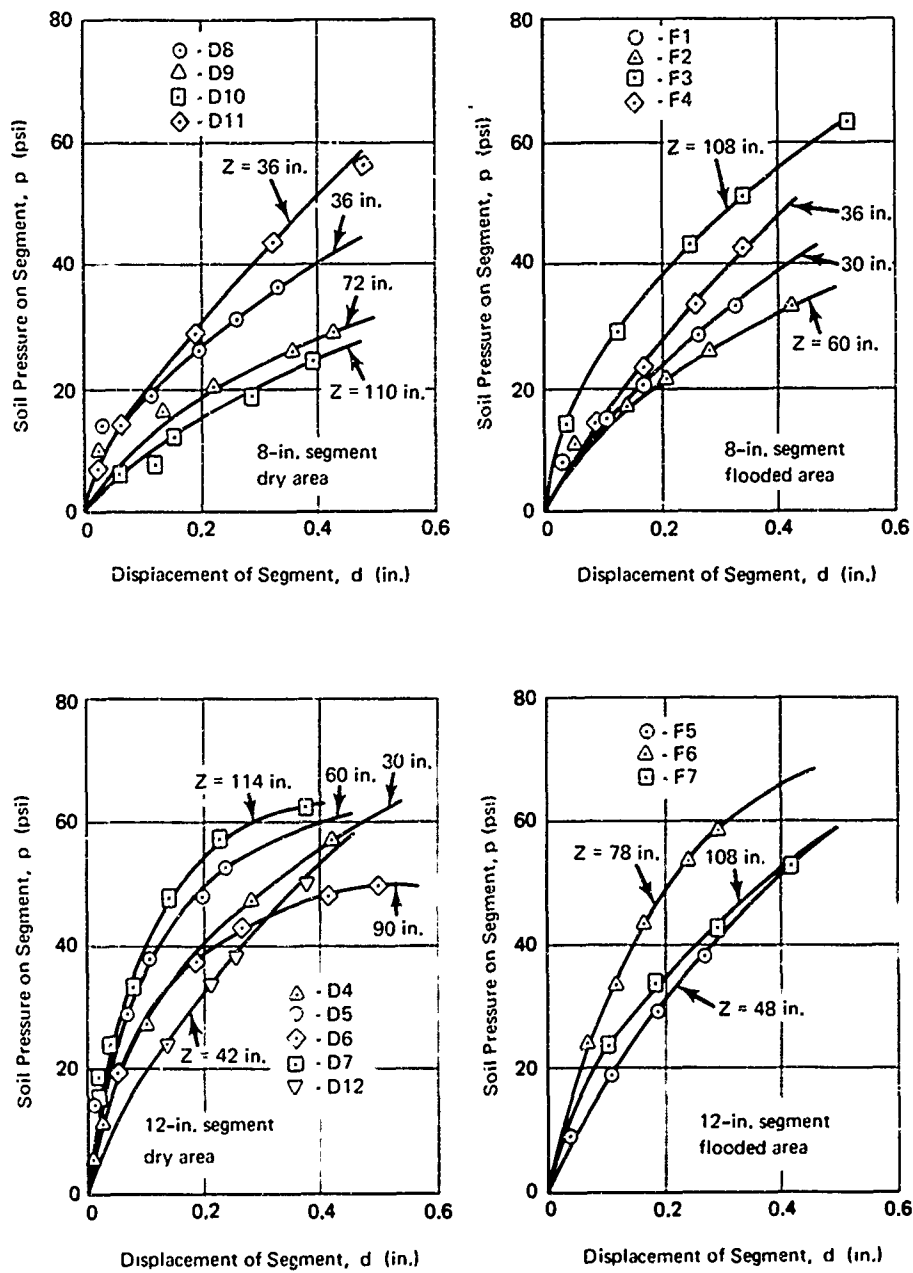


Figure 12. Segmental pile data for El Centro Soil.



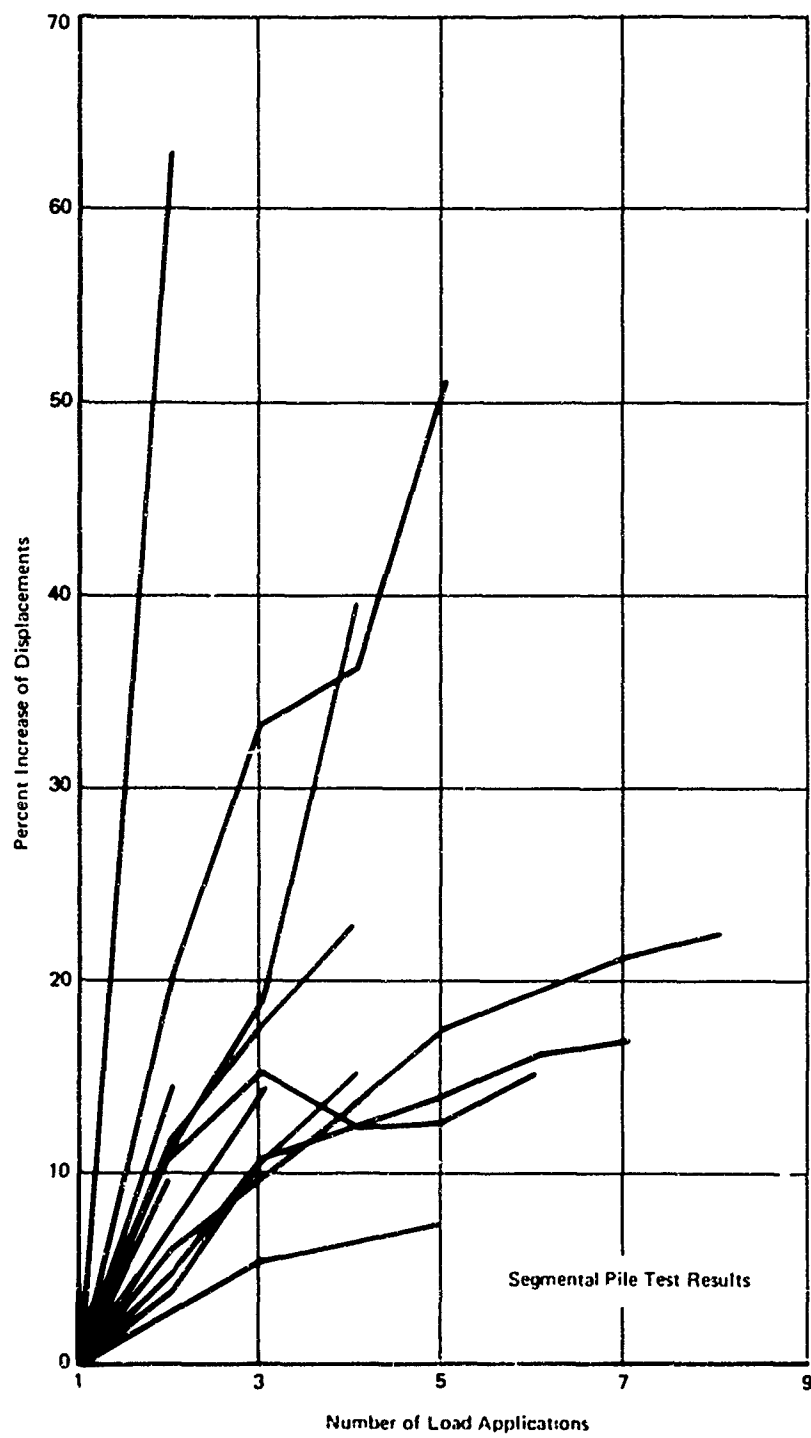


Figure 13. Effect of repetitive loadings on displacements.

It is noted that the segmental pile test data presented in Figure 12 are not presented in a form suitable for application to the general problem of laterally loaded piles. It is necessary to apply scaling relationships and shape factors which have been explained previously.<sup>4</sup> These adjustments are discussed in a later section of the report where the segmental pile test data are used as a guide in the formulation of generally applicable nonlinear horizontal load-displacement relationships for soil.

#### Data from Lateral Load Tests of Piles

Lateral load-displacement curves for the piles tested at El Centro are presented in Figure 14, and similar curves for the slopes at the groundline are presented in Figure 15. It is again pointed out that the lateral load was applied at a point approximately 32 inches above the groundline so that the loading could be resolved to an equivalent groundline moment in addition to a groundline shearing force. The effects of both pile size and soil condition can readily be seen in the plots, and these effects along with the theoretical results illustrated by the solid lines in Figures 14 and 15, are discussed further.

#### THEORETICAL STUDY

The theoretical portion of this program has been associated mainly with the development of procedures for determining the nonlinear lateral load-displacement relationships for natural soil deposits. It has been found that a rectangular hyperbola such as that described earlier provides a satisfactory representation of these relationships.<sup>4</sup> Therefore, the following discussion is devoted to the development of techniques for relating the soil properties and other boundary conditions to the parameters necessary for the definition of a hyperbolic representation of the lateral load-displacement curves.

For the definition of these curves there are two extremely important reference points which must be considered. The first of these is the initial slope,  $k_i$ , of the curves. Guidance in the determination of that quantity can be obtained from constant values of the modulus of horizontal subgrade reaction,  $k_o$ , for preloaded cohesive soils which have been proposed for use in predicting moments in laterally loaded piles.<sup>1,2</sup> The values proposed are based upon the consistency of the soil and are approximately equal to the product of 67 times the undrained shear strength of the soil. Because the proposed values are, by necessity, somewhat conservative, and because the load-displacement curves characteristically exhibit concave downward curvature, it is certain that the initial moduli,  $k_i$ , will be larger than  $67S_u$ .

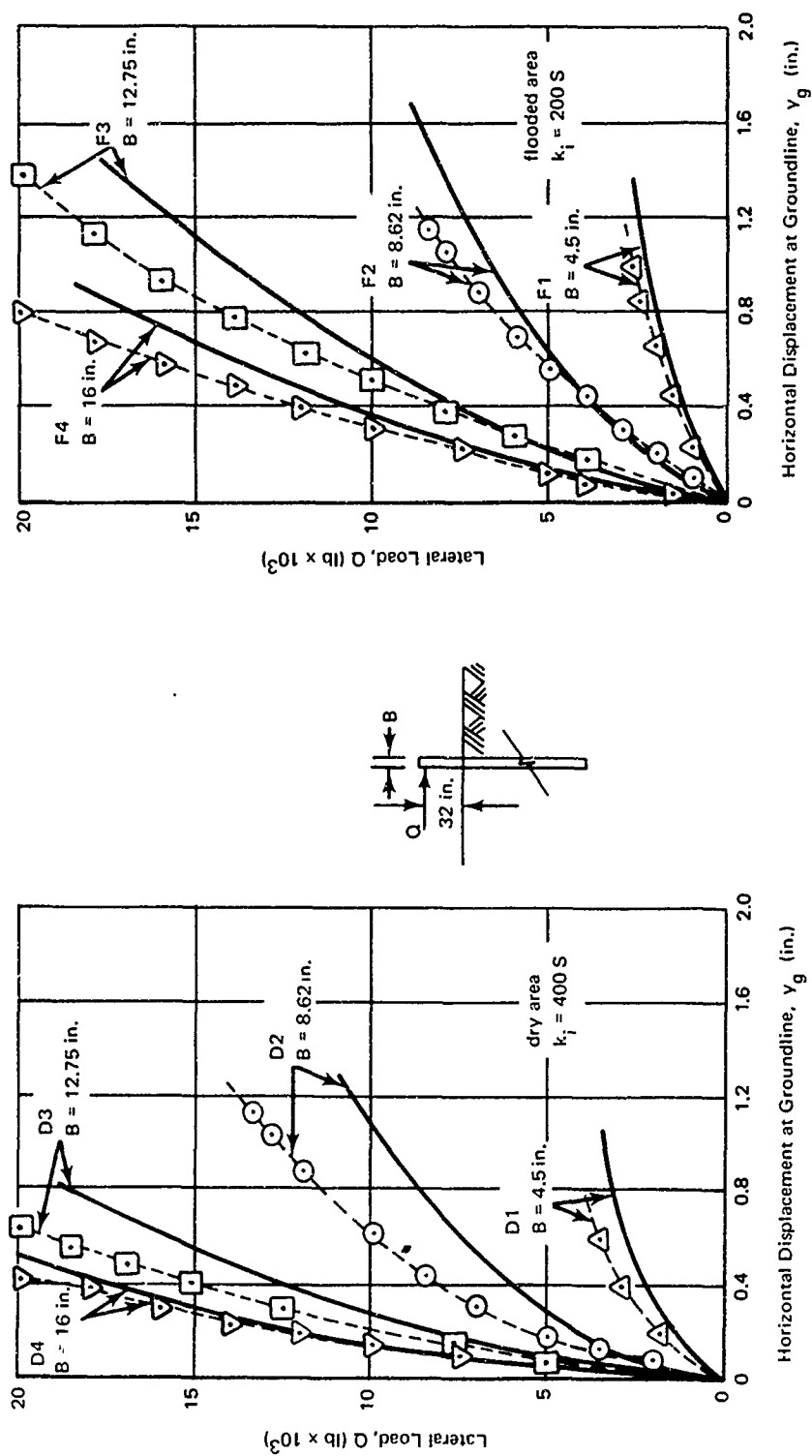


Figure 14. Displacements at the groundline during pile tests at El Centro.  
(Solid lines represent computer solutions.)

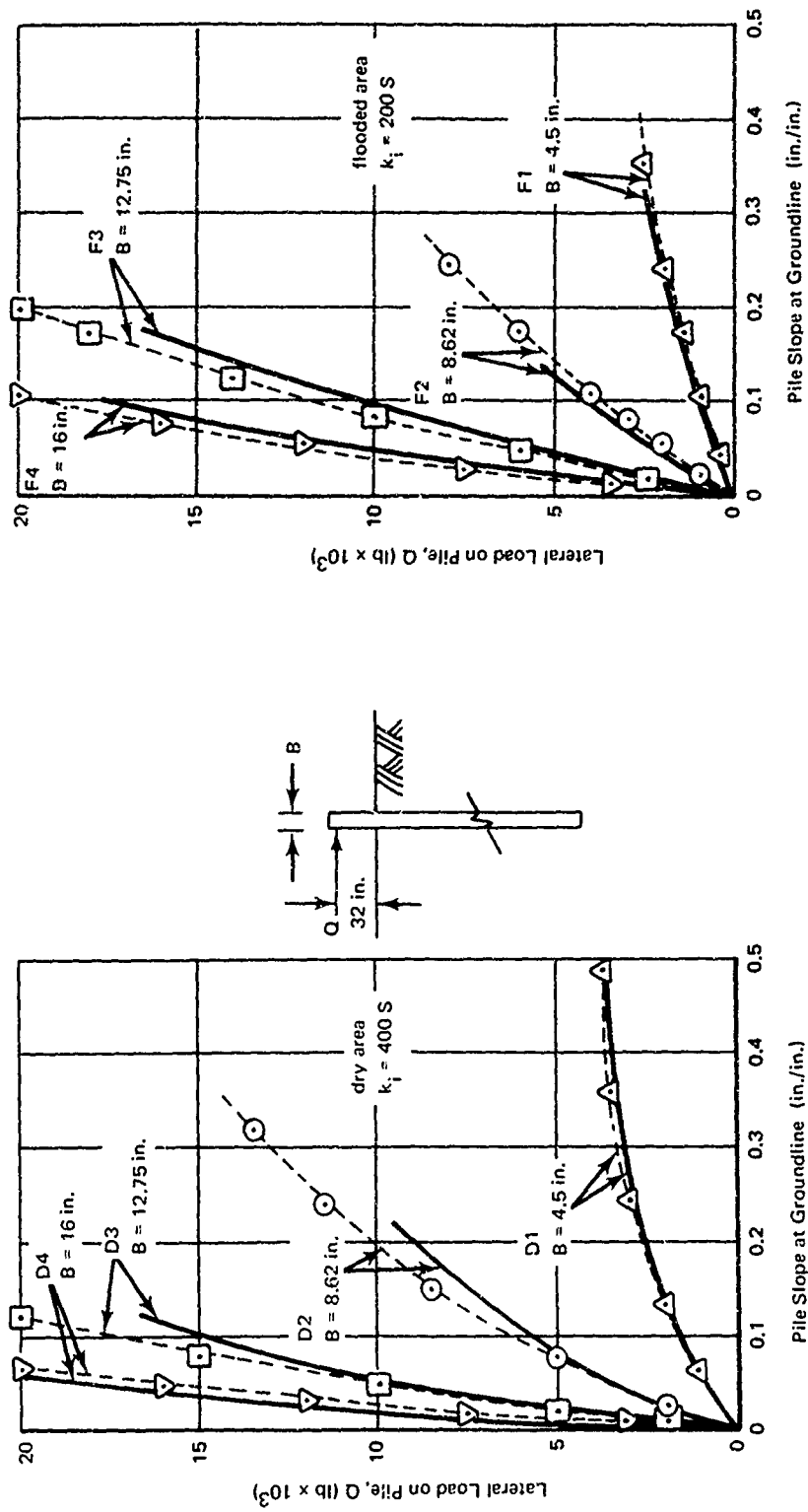


Figure 15. Pile slopes at the groundline during pile tests at El Centro.  
(Solid lines represent computer solutions.)

The other reference point can be obtained by comparing the lateral bearing capacity of the soil,  $p_t$ , to the vertical bearing capacity at corresponding depths. The lateral bearing capacity would be expected to be no larger than the vertical bearing capacity at large depths, and normally  $p_t$  would be considerably smaller than the corresponding vertical values at locations near the ground surface because of the orientation of the respective failure surfaces. Thus, the ratio of  $p_t$  to the undrained shear strength of the cohesive soil would be expected to be a function of depth and, from conventional foundation engineering practice, the ratio would not exceed 9.0 at large depths or 5.5 at shallow depths.

With these two reference points in mind, the El Centro test data were analyzed to determine the proper magnitudes of  $k_i$  and  $p_t$  for the soil at that location. Prior to analyzing the data, though, it was necessary to apply the appropriate factors to account for the size and the shape of the test segments, in order to have the segmental pile test data correspond to the boundary conditions in existence during the lateral load tests on piles. These factors have been discussed in detail in an earlier report.<sup>4</sup> Summarizing the procedure, it is appropriate to plot  $1.5d/pH\alpha$  as a function of  $1.5d/H\alpha$  where  $H$  represents the height of the test segment,  $p$  is the change in the average horizontal soil pressure on the test segment as a result of the corresponding lateral displacement,  $d$ , and  $\alpha$  is a shape factor defined as  $\alpha = 18 \text{ in.}/(12 \text{ in.} + 0.5H)$  for cases where  $H$ , expressed in inches, is equal to or less than 12. It is noted that the quantity 1.5 in the above expression is the assumed magnitude of  $\alpha$  for a laterally loaded pile. With the data expressed in this form, it is possible to determine the appropriate values of  $k_i$  and  $p_t$  from the ordinate intercepts and the slopes of the plots, respectively.

#### Initial Slope of Soil Pressure-Displacement Curves

Hyperbolic plots of the segmental pile test data were made and, in general, the plots were linear so that magnitudes of  $k_i$  and  $p_t$  could be calculated. There was considerable scatter in the values of  $k_i$  obtained, however, it was obvious that the magnitudes of  $k_i$  were considerably larger for the El Centro soil than for the bay mud tested in an earlier program.<sup>4</sup> In addition, there were large differences in the magnitudes of  $k_i$  between the

flooded and the dry locations at El Centro, and the magnitudes of the differences could not be explained solely on the basis of differences in shearing strength of the soil at the two locations. Therefore, it was necessary to do a considerable amount of searching to determine the causes for the differences.

In this search, it was necessary to return to the data from the tests in the bay mud.<sup>4</sup> Both the segmental pile tests and the lateral load tests on piles in that soil were reanalyzed. It was found that the magnitudes of  $k_t$  for that soil were on the order of 100 times the corresponding values of undrained shear strength. The factor of 100 is logical in view of the lower limit of 67S discussed earlier.

Returning to the El Centro data, a similar study of the hyperbolic plots revealed that  $k_t$  was approximately equal to 200S for the flooded area and 400S for the dry area. It is pointed out that the determination of these factors was not a straightforward matter of picking values from the hyperbolic plots. There was such a large amount of scatter in the values of  $k_t/S$ , resulting from the difficulty of experimentally determining the initial slope of a lateral load-displacement curve in soil, that it was required to consider  $k_t$  simultaneously with the magnitudes of  $p_t$ . It should be noted that the measured values of  $p_t$  are relatively precise because they are independent of displacement, whereas the measurements of  $k_t$  require accuracy in both soil pressure and displacement. By working backward from known values of  $p_t$ , it was possible to select values of  $k_t/S$  which were compatible with the measured test data. In that manner, the values of 200 and 400 were determined, and these values were found to be within the range, but conservatively below the mean, of the values of  $k_t$  computed from the hyperbolic plots.

It was found during the study of  $k_t$  that the parameters of the rectangular hyperbola,  $k_t$  and  $p_t$ , could not be determined precisely from the test data. However, it is pertinent that in cases where  $k_t$  was found from a plot to be disproportionately large, the corresponding value of  $p_t$  was found to be disproportionately low. As a result, the use of the factors 200S and 400S for determining  $k_t$ , along with the use of the corresponding expression for  $p_t$  (presented later), provided a realistic representation of the measured soil pressure-displacement curves.

It is pointed out that computed magnitudes of pile response are not very sensitive to changes in the assumed magnitudes of  $k_t$ , therefore, it is not important that  $k_t/S$  be determined accurately. The reason for that lack of sensitivity is suggested in Figure 16 where, for a constant value of  $p_t$ , the limited effect of a relatively large percentage change of  $k_t/S$  on the resulting soil pressure-displacement curves can be seen. A demonstration of the

relatively small influence of changes in  $k_i/S$  appears in Figure 17 where theoretical predictions of pile displacements are presented for two values of the ratio. It can be observed that a doubling of  $k_i/S$  resulted in only about a 22% decrease in the displacements computed.

Possible reasons for the resulting differences in the magnitudes of  $k_i/S$  were investigated. It was suspected that the ratio was related in some manner to the presence of negative pore pressures in the desiccated crust, so a readily determinable measure or index of these pore pressures was sought. It was felt that the liquidity index should exhibit a gross, qualitative-type of relationship to the negative pore pressures, so a plot of liquidity index,  $L_i$  versus  $k_i/S$ , Figure 18, was made. Since neither  $k_i/S$  nor  $L_i$  could be defined with precision, the data were represented as shaded zones rather than data points. An apparent discrepancy exists in the data for the bay mud in that a change in  $L_i$  apparently caused no change in  $k_i/S$ . No attempt is made to explain this discrepancy, however, in view of the general recommendations to follow, the discrepancy is inconsequential.

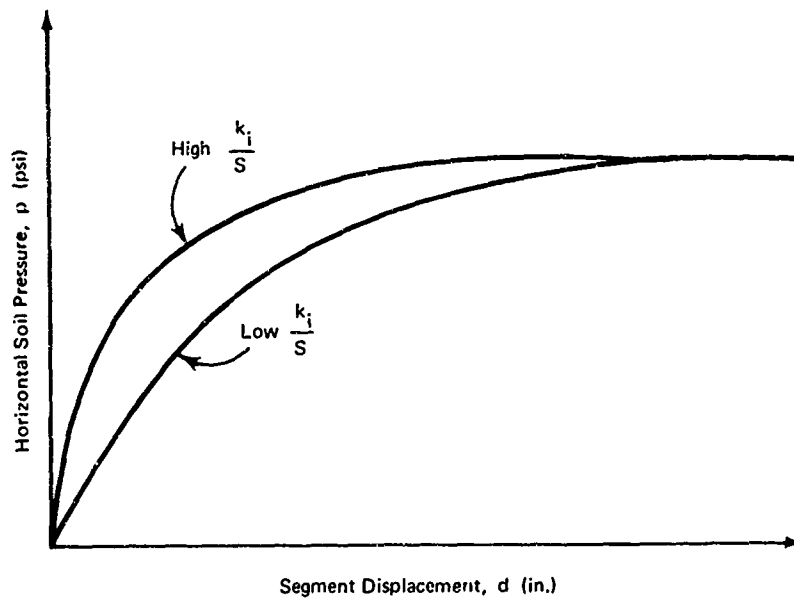


Figure 16. Soil pressure-displacement curves for different soils with similar failure pressures and different initial slopes.

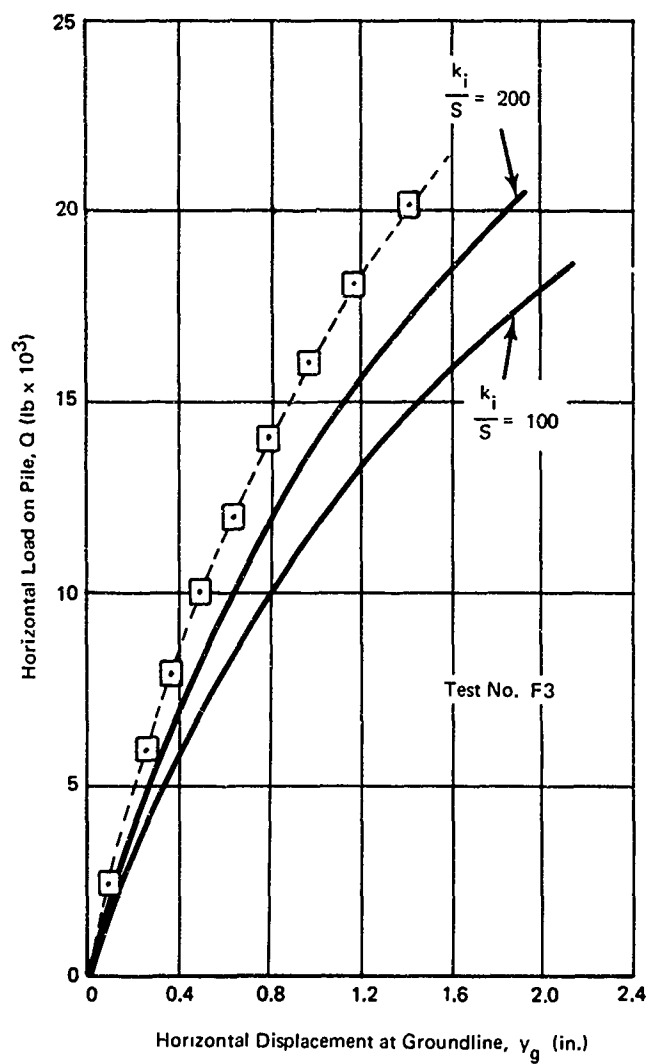


Figure 17. Typical force-pile displacement curves, emphasizing the effect of varying  $k_i/S$  in computer solution.

Based upon the results of the segmental pile tests and the lateral load tests on piles, it is recommended that the magnitude of  $k_i/S$  be taken as 100 for cohesive soils

$$k_i \approx 100S \quad (5)$$



It is recognized that for desiccated clays with a low liquidity index the recommendation will result in overconservative values of computed displacements; however, the test results have indicated that the value of 100 would be approached in such a case if the soil were to become saturated. Thus, the use of a value larger than 100 could prove to be unconservative if a heavy rainstorm or some other phenomenon causing flooding should occur. The use of a value lower than 100 is not warranted because available test data indicate that no lesser values would occur, and that value is realistic in comparison with the lower limit of 67 discussed previously.

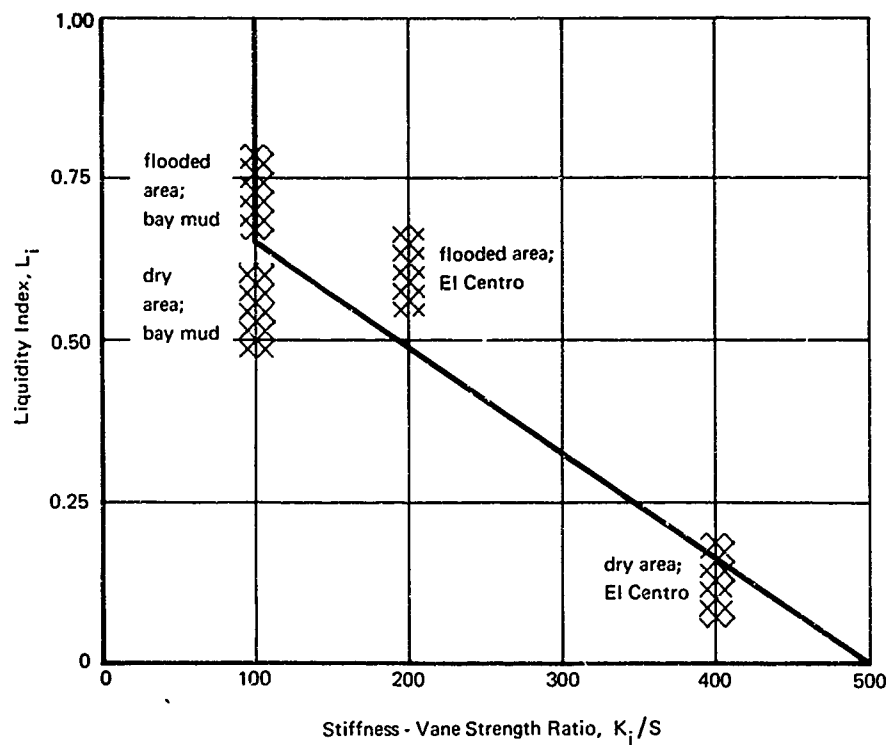


Figure 18. Relationship between hyperbolic parameter and liquidity index.

## Lateral Bearing Capacity

During the determination of an appropriate relationship for the lateral bearing capacity,  $p_f$ , of cohesive soil, it was again necessary to return to the data pertaining to the bay mud, discussed previously in Reference 4. Results of theoretical studies of lateral bearing capacity<sup>13</sup> were used as a guide in the formulation of the relationship for  $p_f$  proposed in Reference 4. It was found that  $p_f$  was directly proportional to  $S$  and  $Z/B$  where  $S$  is the undrained shear strength,  $Z$  is the depth below the ground surface, and  $B$  is the pile width. An investigation of the El Centro data indicated that the same expression for  $p_f$  provided predictions which were within about  $\pm 30\%$  of the measured values. However, it was later found to be necessary to alter the scaling relationship,  $Z/B$ , on the basis of the data from the lateral load tests on piles.

The relationship for  $p_f$  proposed in Reference 4 led to realistic predictions of pile response in the bay mud; however, it was noted that a straight  $Z/B$  scaling resulted in values of  $p_f$  which were too low for 16-inch-diameter piles and slightly high for 4.5-inch-diameter piles. A similar situation was discovered with the El Centro data. Therefore, the theoretical studies were consulted, and it was noted that the assumption of inverse proportionality of  $p_f$  to  $B$  resulted in the pile width having more influence than was appropriate. Consequently, other functions of pile width were investigated, and it was found that the square root of  $B$  was appropriate for the data from the lateral load tests in both the bay mud and the El Centro soil. Thus, the following relationship for  $p_f$  was evolved

$$p_f \approx 0.25 S \left( \frac{Z}{\sqrt{B}} \right) \quad (6)$$

It is noted that Equation 6 is not dimensionally correct. The ramifications of the nondimensionality have been studied, and the conclusion was reached that the resulting equation is only an empirical approximation of a perhaps more complicated dimensionally correct relationship for  $p_f$ . It does, however, provide an expedient means of computing fairly reliable values of lateral bearing capacity for cohesive soils.

One further point which must be mentioned in connection with the expression for  $p_f$  is the reference point alluded to earlier in regard to the maximum possible value of  $p_f/S$ . From Equation 6 it is obvious that the stipulation that  $p_f/S$  at shallow depths could not exceed approximately 5.5 is satisfied. As one would intuitively expect from the orientation of the failure surfaces, that ratio would be far less than the corresponding value for

vertical bearing capacity. Also, it was mentioned earlier that  $p_t/S$  could not exceed approximately 9.0 at great depths. This latter criterion is not met by Equation 6, however, the values of  $Z/\sqrt{B}$  for which  $p_t/S$  exceeds 9.0 are in a zone of soil sufficiently deep that it has only a negligible influence on the response of laterally loaded piles. Therefore, there was no justification in this study for a more elaborate relationship or perhaps a step function for  $p_t$ .

The criteria presented previously have been applied to a large number of cases reported in the literature. In all cases, the proposed criteria have led to conservative results and, in some cases, the computed response proved to be somewhat overconservative. However, there was no indication that the criteria should be altered to account for these conservative results because the soil conditions reported in the literature were not defined as accurately as would have been desirable, especially at the very shallow depths. Frequently, the soil data were in the form of qualitative word descriptions of the consistency of clay, e.g., soft, very soft, medium, etc, or similar descriptions of the relative density of sand, e.g., loose, medium, etc. These descriptions were extrapolated to assumed quantitative values of shear strength parameters, and the resulting errors were apparently large.

Other factors which contributed to the conservative nature of the computed results are associated with the methods used to determine the reported soil properties and with the time at which the properties were measured. Many of the values of consistency of the cohesive soil were based upon the results of unconfined compression tests performed with soil samples obtained with thick-walled samplers. Therefore, the soil samples were undoubtedly disturbed. Other values of consistency of cohesive soils were based upon the results of standard penetration tests, an unreliable procedure for that type of soil.

The effect of the time at which the soil properties were determined is relevant only for the tests in granular soil. It was decided during the experimental program that the prudent approach would be to measure the properties of the granular soil subsequent to the pile driving operations at the site because the pile driving would tend to densify the soil, leading to a stiffer response of the pile. Therefore, if correlations were made on the basis of soil properties determined prior to driving, an unconservative design procedure could result. On the other hand, the approach taken may lead to conservative results, if the soil properties are measured prior to pile driving. For the tests reported in the literature, the properties were measured prior to driving so conservative results were computed.

### Computation of Lateral Soil Pressure-Displacement Diagrams

Earlier discussions have described the procedures used to determine the parameters required to define lateral soil pressure-displacement relationships in terms of soil and pile properties. These relationships are summarized in the following discussion, and similar relationships for granular soil deposits are presented.

**Cohesive Soil.** For a determination of the lateral soil pressure-displacement relationships applicable to cohesive soils, it is necessary to obtain a measurement of the undrained shearing strength to a depth of perhaps 20 pile diameters. These strength values can then be substituted in Equations 5 and 6, repeated below, to determine the necessary parameters for computing the relationships

$$k_i \approx 100S \quad (5)$$

$$p_f \approx 0.25S \left( \frac{Z}{\sqrt{B}} \right) \quad (6)$$

These parameters can in turn be substituted into Equation 3 to provide a convenient representation of the soil pressure-displacement relationship

$$\frac{1}{k} = \frac{y}{pB} = \frac{1}{k_i} + \frac{1}{p_f} \left( \frac{y}{B} \right) \quad (3)$$

**Granular Soil.** For granular soil, the computational procedures are somewhat more complicated than the corresponding procedures for cohesive soils. First, it is necessary to obtain a measure of the angle of internal friction,  $\phi$ , of the soil to a depth of, again, perhaps 20 pile diameters. This can be obtained by triaxial tests or by index measurements of relative density. During earlier tests in a hydraulic fill of granular material, it was found that the vane resistance,  $S$ , in psi (computed as if it were vane shear strength) was approximately equal to the standard penetration resistance,  $N$ , in blows per foot <sup>4</sup> Thus, the following relationship for  $\phi$  was proposed on the basis of available data on standard penetration tests <sup>14, 15</sup>

$$\phi \approx \left( \frac{25.4 - \bar{p}_o}{2.94 + 0.1225 \bar{p}_o} \right) S^{0.16} \quad (S \approx N) \quad (7)$$

It is noted that  $\phi$  is in degrees when  $S$  is in psi and when  $\bar{p}_o$ , the effective overburden pressure, is in psi.

In the earlier work,<sup>4</sup> the relationship of  $\phi$  to  $p_t$  was based entirely upon theory because the segmental pile tests could not be carried to failure of the soil in bearing. However, subsequent comparisons of computed and measured pile response have indicated that the proposed relationships were of approximately the correct form, but the predicted magnitudes of  $p_t$  at shallow depths were too small. Therefore, the original form of the relationship was retained, and the coefficients were altered empirically in order to provide more realistic predictions of lateral bearing capacity at shallow depths. The following relationship resulted

$$p_t \approx \bar{p}_o \left[ 0.664 (10^{0.038 \phi}) + 0.049 (10^{0.034 \phi}) \left( \frac{Z}{B} \right) \right] \quad (8)$$

Here, as before,  $\phi$  is expressed in degrees and  $\bar{p}_o$  is the effective overburden stress.

It was found during the previously reported work that

$$k_i \approx 2,000 \text{ psi} \quad (9)$$

for sand.<sup>4</sup> An analysis of data from lateral load tests on piles reported in the literature has indicated that Equation 9 provides reasonable results. Therefore, the lateral soil pressure-displacement relationships for granular soils can be computed with Equation 3 and the input parameters provided by Equations 7, 8, and 9.

**Repetitive Loadings.** The effects of repetitive and cyclic loadings can be accounted for by adjusting the input soil parameters or by applying correction factors to the computed pile response. The latter procedure has been chosen because the necessary adjustments to the soil parameters could lead to erroneous predictions of moments in the piles.

Cyclic or repetitive loadings have the effect of increasing a pile displacement at a decreasing rate with increasing numbers of cycles or repetitions. This results from either remolding an undisturbed cohesive soil or densifying a granular soil by the process of repeated shearing deformations. The results of field and model tests, as summarized by Prakash,<sup>16</sup> indicate a 20 to 50% increase in groundline displacement for infinite repetitions of a constant load in granular and cohesive soils. The cohesive soils tested, however, were insensitive clays. Little is known of the effects of repetitive pile loads on sensitive clays and a discussion thereof is excluded. More research is needed in the area.

Repetitive load tests were performed with the segmental pile, and the results of these tests were shown in Figure 13. Similar results from earlier tests with the segmental pile in bay mud have been reported.<sup>4</sup> These latter data indicate percentage increases in the vicinity of the upper limit of the range proposed by Prakash, so it is recommended that a 50% increase of displacements be assumed for conditions of cyclic or repetitive loadings.

An investigation of the effects of repetitive and cyclic loadings on the magnitudes of maximum moments in the piles indicated that there was negligible danger of a moment increase in a pile during these additional loadings.

### Computed Pile Response

**Computational Procedure** Equation 2 was solved by an iterative finite difference procedure explained in an earlier report.<sup>4</sup> For this study, the computer program was refined somewhat, and the lateral soil pressure-displacement parameters presented in the preceding sections were incorporated. The proposed final version of the computer program is presented in the Appendix.

For each computation, the appropriate soil properties and pile boundary conditions were provided as input to the program. The results obtained were in the form of a tabulation of horizontal displacement, bending moment, soil pressure, and modulus of horizontal subgrade reaction at several points along the embedded length of the pile.

**Computer Solutions.** The data measured during the lateral load tests on piles consisted of lateral displacements and slopes of the pile at the level of the ground surface for various magnitudes of lateral loads. Bending moments as a result of the load applications above the ground surface were accounted for in the computations. Computed magnitudes of displacement and slope are presented in Figures 14 and 15, respectively, for the tests at El Centro. For these computations, values of  $k$ , equal to 400S and 200S were used for the dry location and the flooded location, respectively. It can be seen that the computed results are, with few exceptions, somewhat conservative.

Because the previously reported results of tests in the bay mud and the hydraulic fill have been referred to frequently in this report, a comparison of computed and measured horizontal displacements during tests in these soils is provided in Figures 19 and 20, respectively. Again, the computer solutions have provided sufficiently conservative results.

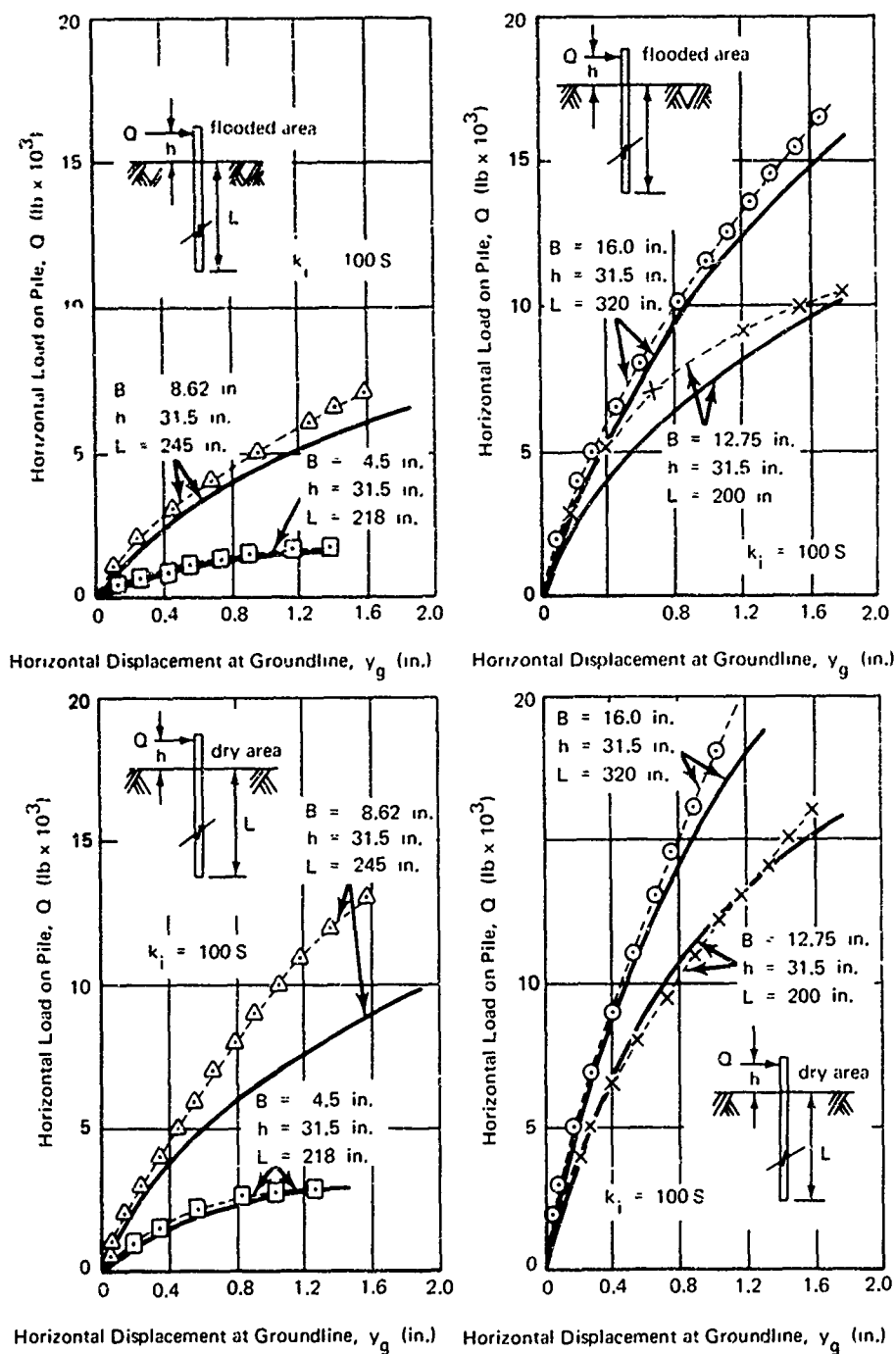


Figure 19. Lateral load-displacement curves from pile tests in bay mud.  
(Computer solutions are represented by solid lines.)

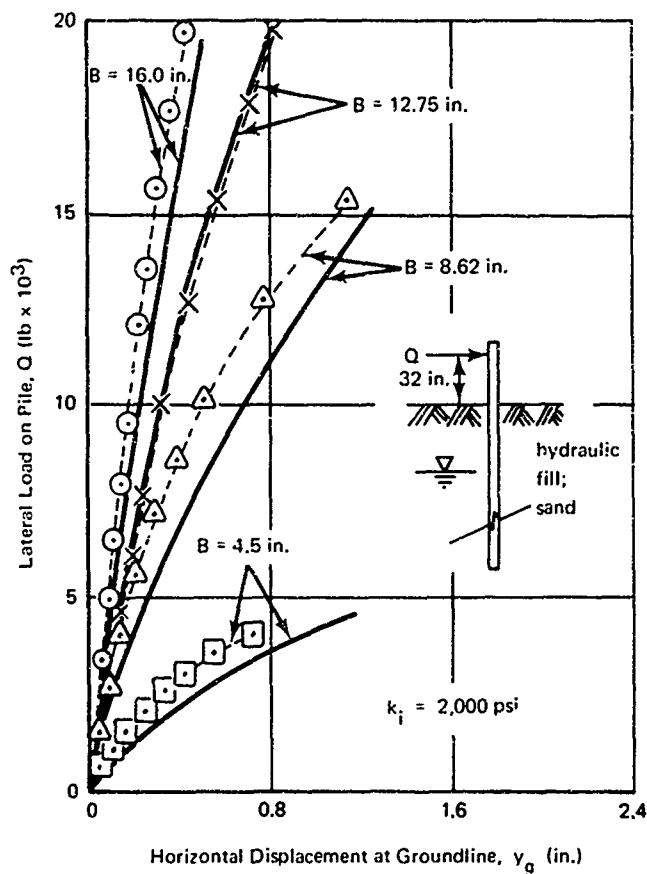


Figure 20. Results of lateral load tests on piles in the hydraulic fill.

#### TABULAR SOLUTION FOR laterally LOADED PILES

There are many cases where it is desirable to have a reasonably accurate solution of the laterally loaded pile problem with nonlinear soil behavior being considered, but in most of those cases it is not possible or economical to obtain access to a computer and a computer program of the type listed in the Appendix. In such cases, it is possible to utilize a more approximate method of computation which has been developed during this study. This method utilizes the nonlinear soil pressure-displacement relationships presented earlier, while computing an approximate variation of the modulus of horizontal subgrade reaction,  $k$ , with depth. These magnitudes of  $k$  can then be substituted into existing design charts, and pile response can be estimated.



During the computer study discussed earlier, it was noted that in all cases, the computed variations of  $k$  with depth could be approximated reasonably with the well-known function

$$k = n_h Z \quad (10)$$

where  $n_h$  is a constant of horizontal subgrade reaction. Equation 10 was reasonable even for the deposits of cohesive soil with a desiccated surface layer. Thus, it was possible to develop a procedure for estimating an appropriate value of  $n_h$  for a given pile in a deposit of either cohesive or noncohesive soil for a given condition and magnitude of loading. It is noted that, even though  $k$  was assumed to be directly proportional to depth, similar design procedures can easily be developed with other assumed variations such as step functions or exponential functions

There are several steps involved in the hand solution, and these steps are described before they are presented in tabular form.

1. Assume a trial value of  $n_h$  for the soil. It has been found that by assuming a value of  $n_h$  larger than the anticipated actual value, convergence is obtained more rapidly than by assuming lower values. Therefore, an assumed value of 50 lb/in.<sup>3</sup> for  $n_h$  is recommended.

2. Compute a trial value of a relative stiffness factor,  $T$ , defined as follows

$$T = \left( \frac{EI}{n_h} \right)^{0.2} \quad (11)$$

where  $EI$  is the flexural stiffness of the pile

3. Determine the necessary soil properties at several depths along the length of the pile, and give added weight to the soil at shallow depths in a manner similar to that shown later in Table 3. For cohesive soils, a knowledge of the undrained shear strength at those depths is required. For granular soils, the angle of internal friction,  $\phi$ , or an index thereof (Equation 7), and the effective overburden pressure,  $\bar{p}_o$ , are required.

4. With the values of  $EI$  and  $n_h$  assumed for the first trial, compute trial values of pile displacements at the depths for which soil properties were determined. These computations can be made with the use of procedures which have been proposed for granular soils.<sup>8</sup> The resulting design charts have been presented in a Navy Design Manual.<sup>17</sup>

5. With the trial displacements in conjunction with the measured soil properties, compute a corresponding value of the modulus of horizontal subgrade reaction,  $k$ , at each depth with Equation 3. For cohesive soils, Equations 5 and 6 can be used; and for granular soils, Equations 7, 8, and 9 are applicable.

6. A plot of  $k$  versus depth can be made to determine the next trial value of  $n_h$  or, if necessary, another more appropriate distribution of  $k$  with depth can be determined. In the tabular solution, a procedure is presented for computing the next trial value of  $n_h$  without the necessity of making a plot of  $k$  versus  $Z$ .

7. Using the next trial value of  $n_h$ , repeat steps 2 through 6. Perform a sufficient number of iterations that the resulting displacements are approximately the same from one trial to another.

8. With the final trial value of  $n_h$ , compute such other pile response parameters as are necessary by using the available design charts.<sup>17</sup>

For the tabular solution, an expediency was developed to allow the computation of trial average values of  $n_h$  (step no. 6) without the requirement of a plot of  $k$  versus  $Z$ . It was recognized that the computed values of  $k$  for the zone of soil near the ground surface would have more influence on the behavior of a laterally loaded pile than would those values for depths near the point of inflection of the displaced pile. It was noted also that the point of inflection typically occurs at a depth equivalent to slightly less than  $2T$ . Therefore, depths for which computations of  $k$  are to be made were defined in terms of  $T$ , and the concentration of depths for computations was specified to diminish with depth. At each depth a corresponding value of  $n_h$  can be computed with the trial value of  $k$  and with Equation 10; a simple arithmetic mean of the resulting values of  $n_h$  provides the desired weighted average.

Initially, reasonable values of depth in terms of  $T$  were determined intuitively. Trial solutions then were compared with the more exact computer solutions using the program presented in the Appendix. Minor adjustments to the specified values of depth were made on the basis of the resulting comparisons, and the established values are presented in Table 3. The values of  $A_y$  and  $B_y$  were taken from design curves in the Navy Design Manual<sup>17</sup> for an infinitely long pile. Therefore, if those values of  $A_y$  and  $B_y$  are used, each trial solution should be checked to ensure that the pile length is greater than  $4T$ .<sup>8</sup> It was found from this study that the proposed tabular solution resulted in computed pile response data with sufficient accuracy, in comparison with the computer solutions, that the computer solutions can be supplanted in most typical cases.

Table 3. Tabular Form of Computational Procedure

Trial No. _____		$T = \left( \frac{EI}{n_h} \right)^{0.2} = \text{_____ in.}$					$B = \text{_____ in.}$			
Depth, $\left( \frac{Z}{T} \right)$	Depth, Z (in.)	$A_y$	$Y_Q = A_y \left( \frac{Q_g T^3}{EI} \right)$ (in.)	$B_y$	$Y_m = B_y \left( \frac{M_g T^2}{EI} \right)$ (in.)	$Y = Y_Q + Y_m$ (in.)	$P_f$ (psi)	$k_i$ (psi)	$k = \frac{1}{\frac{1}{k_i} + \frac{1}{p_f B}}$ (psi)	$n_h = \frac{k}{Z}$ (psi)
0.00		2.40		1.60						
0.05		2.32		1.52						
0.10		2.25		1.45						
0.30		1.90		1.10						
0.55		1.55		0.80						
0.90		1.15		0.40						
1.40		0.45		0.10						
2.80		0.10		0.15						

$T =$  relative stiffness factor  
 $EI =$  flexural stiffness of pile  
 $n_h =$  constant of horizontal subgrade reaction  
 $B =$  pile width

$Q_g =$  \_\_\_\_\_ lb  
 $M_g =$  \_\_\_\_\_ in.-lb  
Soil = \_\_\_\_\_  
  
Total  $n_h =$  \_\_\_\_\_  
Average  $n_h = \frac{\text{Total}}{7.0} =$  \_\_\_\_\_

It is noted that each tabular solution provides a value of  $n_h$  which is applicable only for the specific loading condition considered. For other loading conditions, a different value of  $n_h$  would result if all other pile and soil conditions remained the same. This behavior (as a result of the nonlinear soil response) is demonstrated in the following example problem.

#### Example Problem

In this example problem, an actual field test is utilized in order that a comparison between computer results, results of tabular solutions, and measured test data are available. Test No. P4 is considered. The pile properties are as follows:

Width, B = 16 in.  
Stiffness, EI =  $1.69 \times 10^{10}$  lb-in.<sup>2</sup>  
Length, L = 324 in.

A profile of vane resistance versus depth was presented in Figure 10 and, because the test was performed in the dry location at El Centro, the larger values of  $S$  are appropriate. Two levels of horizontal load, 10,000 and 15,000 pounds are considered, along with the moments resulting from the 31-inch-height of the point of application of the loads.

Because a comparison of theoretical and experimental results is being made, values of  $k_i = 400S$  are used in both the tabular solution and the computer solution instead of the suggested design value of  $100S$  indicated in Equation 5. In both cases, the values of  $p_i$  are predicted with Equation 6.

It was mentioned during the preceding discussion of the tabular solution that relatively rapid convergence can be achieved by assuming an initial trial value of  $n_h$  greater than the anticipated actual value. It has been found that essentially the same final solutions result regardless of the initial assumption of  $n_h$ ; therefore, a low value of  $n_h$ , 10 lb/in.<sup>3</sup>, is used in this example problem in order to provide a demonstration of the relatively rapid convergence resulting even with a poor assumption of  $n_h$ .

The entire tabular solution is presented in Table 4. Nine iterations were performed although there was very little change in the computed displacements after the fifth iteration. The resulting value of 0.18 inch for the displacement at the groundline is compared in Table 5 with the corresponding value computed with the computer program listed in the Appendix. The displacement measured during the field test is presented also. It is pointed out that the comparison between the two computed values is not as good as is usually found; in that regard, the percentage difference between the two computed values for a load level of 15,000 pounds is somewhat better.

Table 4. Tabular Form of Computational Procedure

Trial No. 1		$T = \left( \frac{EI}{\eta_h} \right)^{0.2} = 70 \text{ in.}$					$B = 16 \text{ in.}$			
Depth, $\left( \frac{Z}{T} \right)$	Depth, $Z$ (in.)	$A_y$	$y_0 = A_y \left( \frac{Q_g T^3}{EI} \right)$ (in.)	$B_y$	$y_m = B_y \left( \frac{M_g T^2}{EI} \right)$ (in.)	$y = y_0 + y_m$ (in.)	$p_f$ (psi)	$k_i$ (psi)	$k = \frac{1}{\frac{1}{k_i} + \frac{1}{p_f B}}$ (psi)	$\eta_h = \frac{k}{Z}$ (psi)
0.00	0.0	2.40	0.48	1.60	0.14	0.63	0.0	3,500	0	0.0
0.05	3.5	2.32	0.47	1.52	0.13	0.60	39	7,109	101	28.7
0.10	7.0	2.25	0.45	1.45	0.13	0.58	11.7	10,718	310	44.1
0.30	21.0	1.90	0.38	1.10	0.09	0.48	29.5	8,977	876	41.6
0.55	38.5	1.55	0.31	0.80	0.07	0.38	37.5	6,224	1,239	32.1
0.90	63.0	1.15	0.23	0.40	0.03	0.27	43.1	4,376	1,613	25.6
1.40	98.1	0.45	0.09	0.10	0.00	0.10	71.4	4,657	3,302	33.6
2.80	196.2	0.10	0.02	0.15	0.01	0.03	166.8	5,442	5,090	25.9

$T = \text{relative stiffness factor}$   
 $EI = \text{flexural stiffness of pile}$   
 $\eta_h = \text{constant of horizontal subgrade reaction}$   
 $B = \text{pile width}$

$Q_g = 10,000 \text{ lb}$   
 $M_g = 310,000 \text{ in.-lb}$   
 $\text{Soil} = \text{Cohesive}$

$\text{Total } \eta_h = 231.7$   
 $\text{Average } \eta_h = \frac{\text{Total}}{7.0} = 33.1$

Continued

Table 4. Tabular Form of Computational Procedure (Contd)

Trial No. 2										
$T = \left(\frac{EI}{n_h}\right)^{0.2} = 55 \text{ in.}$										
$B = 16 \text{ in.}$										
Depth, $\left(\frac{Z}{T}\right)$	Depth, $Z$ (in.)	$A_y$	$y_Q = A_y \left(\frac{Q_g T^3}{EI}\right)$ (in.)	$B_y$	$y_m = e_y \left(\frac{M_g T^2}{EI}\right)$ (in.)	$y = y_Q + y_m$ (in.)	$p_f$ (psi)	$k_i$ (psi)	$k = \frac{1}{\frac{1}{k_i} + \frac{1}{p_f B}}$ (psi)	$n_h = \frac{k}{Z}$ (psi)
0.00	0.0	2.40	0.23	1.60	0.08	0.32	0.0	3,500	0	0.0
0.05	2.7	2.32	0.23	1.52	0.08	0.31	2.7	6,340	136	49.0
0.10	5.5	2.25	0.22	1.45	0.08	0.30	7.9	9,180	398	72.0
0.30	16.5	1.90	0.18	1.10	0.06	0.24	25.7	9,927	1,409	85.1
0.55	30.3	1.55	0.15	0.80	0.04	0.19	33.2	7,002	1,936	63.8
0.90	49.6	1.15	0.11	0.40	0.02	0.13	55.0	7,088	3,376	68.0
1.40	77.2	0.45	0.04	0.10	0.00	0.05	54.2	4,490	3,562	46.1
2.80	154.4	0.10	0.00	0.15	0.00	0.01	123.2	5,107	4,876	31.6
T = relative stiffness factor					$Q_g = 10,000 \text{ lb}$		Total $n_h = 415.8$			
EI = flexural stiffness of pile					$M_g = 310,000 \text{ in. lb}$		Average $n_h = \frac{\text{Total}}{7.0} = 59.4$			
$n_h = \text{constant of horizontal subgrade reaction}$					Soil = Cohesive					
B = pile width										

Continued

Table 4. Tabular Form of Computational Procedure (Contd)

Trial No 3		$T = \left( \frac{EI}{n_h} \right)^{0.2} = 49 \text{ in.}$						$B = 16 \text{ in.}$		
Depth, $\left( \frac{Z}{T} \right)$	Depth, $Z$ (in.)	$A_y$	$v_Q = A_y \left( \frac{Q_g^{1.3}}{EI} \right)$ (in.)	$B_y$	$v_m = B_y \left( \frac{M_g T^2}{EI} \right)$ (in.)	$y = v_Q + v_m$ (in.)	$p_t$ (psi)	$k_t$ (psi)	$k = \frac{1}{\frac{1}{k_t} + \frac{1}{p_t B}}$ (psi)	$n_h = \frac{k}{Z}$ (psi)
0.00	0.0	2.40	0.16	1.60	0.07	0.23	0.0	3500	0	0.0
0.05	2.4	2.32	0.16	1.52	0.06	0.22	2.3	6,027	157	63.7
0.10	4.9	2.25	0.15	1.45	0.06	0.22	6.6	8,554	449	91.4
0.30	14.7	1.90	0.13	1.10	0.04	0.18	237	10,314	1,739	118.1
0.55	26.9	1.55	0.10	0.80	0.03	0.14	325	7,712	2,464	91.3
0.90	44.1	1.15	0.08	0.40	0.01	0.09	49.4	7,160	3,792	85.8
1.40	68.6	0.45	0.03	0.10	0.00	0.03	47.5	4,422	3,658	53.2
2.80	137.3	0.10	0.00	0.15	0.00	0.01	106.7	4,971	4,782	34.8
T = relative stiffness factor		$Q_g = 10,000 \text{ lb}$		Total $n_h$		- 538.4				
EI = flexural stiffness of pile		$M_g = 310,000 \text{ in.-lb}$		Average $n_h = \frac{\text{Total}}{7.0}$		76.9				
$n_h = \text{constant of horizontal subgrade reaction}$		Soil = Cohesive								
B = pile width										

Continued

Table 4. Tabular Form of Computational Procedure (Contd)

Trial No. 4		$T = \left(\frac{EI}{\eta_h}\right)^{0.2} = 46 \text{ in.}$					$B = 16 \text{ in.}$			
Depth, $\left(\frac{Z}{T}\right)$	Depth, $Z$ (in.)	$A_y$	$v_Q = A_y \left(\frac{Q_g T^3}{EI}\right)$ (in.)	$B_y$	$v_m = B_y \left(\frac{M_g T^2}{EI}\right)$ (in.)	$v = v_Q + v_m$ (in.)	$p_t$ (psi)	$k_i$ (psi)	$k = \frac{1}{\frac{1}{k_i} + \frac{1}{p_t B}}$ (psi)	$\eta_h = \frac{k}{Z}$ (psi)
0.00	0.0	2.40	0.14	1.60	0.06	0.20	0.0	3,500	0	0.0
0.05	2.3	2.32	0.13	1.52	0.06	0.19	2.1	5,900	167	71.5
0.10	4.6	2.25	0.13	1.45	0.05	0.19	6.0	8,300	474	101.4
0.30	13.9	1.90	0.11	1.10	0.04	0.15	22.9	10,471	1,901	135.9
0.55	25.6	1.55	0.09	0.80	0.03	0.12	32.0	8,000	2,716	105.9
0.90	41.9	1.15	0.06	0.40	0.01	0.08	44.5	6,790	3,754	89.5
1.40	65.2	0.45	0.02	0.10	0.00	0.03	44.8	4,394	3,694	56.6
2.80	130.4	0.10	0.00	0.15	0.00	0.01	100.2	4,916	4,742	36.3
T = relative suffness factor		$Q_g = 10,000 \text{ lb}$		Total $\eta_h = 597.3$						
EI = flexural stiffness of pile		$M_g = 310,000 \text{ in.-lb}$		Average $\eta_h = \frac{\text{Total}}{7.0} = 85.3$						
$\eta_h = \text{constant of horizontal subgrade reaction}$		Soil = Cohesive								
B = pile width										

Continued



Table 4 Tabular Form of Computational Procedure (Contd)

Trial No 5										
$T = \left( \frac{EI}{\eta_h} \right)^{0.2} = 45 \text{ in.}$										
$B = 16 \text{ in.}$										
Depth, $\left( \frac{Z}{T} \right)$	Depth, $Z$ (in.)	$A_y$	$\gamma_Q = A_y \left( \frac{Q_g T^3}{EI} \right)$ (in.)	$B_y$	$\gamma_m = B_y \left( \frac{M_g T^2}{EI} \right)$ (in.)	$\gamma = \gamma_Q + \gamma_m$ (in.)	$p_f$ (psi)	$k_i$ (psi)	$k = \frac{1}{\frac{1}{k_i} + \frac{1}{p_f B}}$ (psi)	$\eta_h = \frac{k}{Z}$ (psi)
0.00	0.0	2.40	0.13	1.60	0.06	0.19	0.0	3,500	0	0.0
0.05	2.2	2.32	0.13	1.52	0.05	0.18	2.1	5,850	172	749
0.10	4.5	2.25	0.12	1.45	0.05	0.18	5.8	8,201	484	105.8
0.30	13.6	1.90	0.10	1.10	0.04	0.14	22.5	10,532	1,968	143.7
0.55	25.1	1.55	0.08	0.80	0.03	0.11	31.8	8,112	2,820	112.2
0.90	41.0	1.15	0.06	0.40	0.01	0.07	42.6	6,646	3,736	90.9
1.40	63.8	0.45	0.02	0.10	0.00	0.02	43.8	4,383	3,707	58.0
2.80	127.7	0.10	0.00	0.15	0.00	0.01	97.7	4,894	4,726	37.0

$T = \text{relative stiffness factor}$   
 $EI = \text{flexural stiffness of pile}$   
 $\eta_h = \text{constant of horizontal subgrade reaction}$   
 $B = \text{pile width}$

$Q_g = 10,000 \text{ lb}$   
 $M_g = 310,000 \text{ in. lb}$   
 $\text{Soil} = \text{Cohesive}$

$\text{Total } \eta_h = 622.7$   
 $\text{Average } \eta_h = \frac{\text{Total}}{7.0} = 89.0$

Continued

Table 4. Tabular Form of Computational Procedure (Contd)

Trial No. 6		$T = \left( \frac{EI}{\eta_h} \right)^{0.2} = 45 \text{ m.}$					$B = 16 \text{ m}$			
Depth, $\left( \frac{Z}{T} \right)$	Depth, Z (m.)	$A_y$	$y_Q = A_y \left( \frac{Q_g T^3}{EI} \right)$ (m.)	$B_y$	$y_m = B_y \left( \frac{M_g T^2}{EI} \right)$ (m.)	$y = y_Q + y_m$ (m.)	$p_l$ (psi)	$k_l$ (psi)	$k$ $\frac{1}{\frac{1}{k_l} + \frac{1}{p_l B}}$ (psi)	$\eta_h = \frac{k}{2}$ (psi)
0.00	0.0	2.40	0.13	1.60	0.06	0.19	0.0	3,500	0	0.0
0.05	2.2	2.32	0.12	1.52	0.05	0.18	2.1	5,831	174	76.4
0.10	4.5	2.25	0.12	1.45	0.05	0.17	5.8	8,162	488	107.6
0.30	13.5	1.90	0.10	1.10	0.04	0.14	22.4	10,556	1,996	146.9
0.55	24.8	1.55	0.08	0.80	0.03	0.11	31.7	8,156	2,862	114.9
0.90	40.7	1.15	0.06	0.40	0.01	0.07	41.9	6,589	3,729	91.5
1.40	63.3	0.45	0.02	0.10	0.00	0.02	43.4	4,379	3,712	58.6
2.80	126.7	0.10	0.00	0.15	0.00	0.01	96.8	4,886	4,720	37.2
T = relative stiffness factor		$Q_g = 10,000 \text{ lb}$		Total $\eta_h = 633.2$						
EI = flexural stiffness of pile		$M_g = 310,000 \text{ in lb}$		Average $\eta_h = \frac{\text{Total}}{7.0} = 90.4$						
$\eta_h = \text{constant of horizontal subgrade reaction}$		Soil = Cohesive								
B = pile width										

Continued

Table 4. Tabular Form of Computational Procedure (Contd)

Trial No 7		$T = \left( \frac{EI}{n_h} \right)^{0.2} = 45 \text{ in.}$					$B = 16 \text{ in.}$			
Depth, $\left( \frac{Z}{T} \right)$	Depth, Z (in.)	$A_y$	$y_Q = A_y \left( \frac{Q_g T^3}{EI} \right)$ (in.)	$B_y$	$y_m = B_y \left( \frac{M_g T^2}{EI} \right)$ (in.)	$y = y_Q + y_m$ (in.)	$p_f$ (psi)	$k_f$ (psi)	$k = \frac{1}{\frac{1}{k_f} + \frac{y}{p_f B}}$ (psi)	$n_h = \frac{k}{Z}$ (psi)
0.00	0.0	2.40	0.13	1.60	0.05	0.19	0.0	3,500	0	0.0
0.05	2.2	2.32	0.12	1.52	0.05	0.18	2.0	5,823	174	769
0.10	4.5	2.25	0.12	1.45	0.05	0.17	5.7	8,146	490	108.3
0.30	13.5	1.90	0.10	1.10	0.04	0.14	22.3	10,566	2,007	148.2
0.55	24.8	1.55	0.08	0.80	0.02	0.11	31.7	8,174	2,879	116.0
0.90	40.6	1.15	0.06	0.40	0.01	0.07	41.6	6,567	3,726	91.7
1.40	63.1	0.45	0.02	0.10	0.00	0.02	43.2	4,377	3,714	58.8
2.80	126.3	0.10	0.00	0.15	0.00	0.01	96.4	4,882	4,718	37.3

$T =$  relative stiffness factor  
 $EI =$  flexural stiffness of pile  
 $n_h =$  constant of horizontal subgrade reaction  
 $B =$  pile width

$Q_g = 10,000 \text{ lb}$   
 $M_g = 310,000 \text{ in. lb}$   
Soil = Cohesive

Total  $n_h = 637.4$   
Average  $n_h = \frac{\text{Total}}{7.0} = 91.1$

Continued

Table 4. Tabular Form of Computational Procedure (Contd)

Trial No. 8								
$T = \left( \frac{EI}{n_h} \right)^{0.2} = 45 \text{ in.}$								
$B = 16 \text{ in.}$								
Depth, $\left( \frac{Z}{T} \right)$	Depth, $Z$ (in.)	$A_y$	$y_Q = A_y \left( \frac{Q_g T^3}{EI} \right)$ (in.)	$B_y$	$y_m = B_y \left( \frac{M_g T^2}{EI} \right)$ (in.)	$y = y_Q + y_m$ (in.)	$p_f$ (psi)	$k_f$ (psi)
								$k = \frac{1}{\frac{1}{k_1} + \frac{1}{p_f B}}$ (psi)
								$n_h = \frac{k}{Z}$ (psi)
0.00	0.0	2.40	0.12	1.60	0.05	0.18	0.0	0
0.05	2.2	2.32	0.12	1.52	0.05	0.18	2.0	174
0.10	4.5	2.25	0.12	1.45	0.05	0.17	5.7	490
0.30	13.5	1.90	0.10	1.10	0.04	0.14	22.3	2,012
0.55	24.7	1.55	0.08	0.80	0.02	0.11	31.7	2,886
0.90	40.5	1.15	0.06	0.40	0.01	0.07	41.5	3,724
1.40	63.0	0.45	0.02	0.10	0.00	0.02	43.1	3,715
2.80	126.1	0.10	0.00	0.15	0.00	0.01	96.2	4,717
T = relative stiffness factor					$Q_g = 10,000 \text{ lb}$	Total $n_h$ 639.1		
EI = flexural stiffness of pile					$M_g = 310,000 \text{ in.-lb}$			
$n_h = \text{constant of horizontal subgrade reaction}$					Soil = Cohesive	Average $n_h = \frac{\text{Total}}{7.0} = 91.3$		
B = pile width								

Continued

Table 4. Tabular Form of Computational Procedure (Contd)

Trial No. 9										
$T = \left( \frac{EI}{n_h} \right)^{0.2} = 45 \text{ in.}$										
$B = 16 \text{ in.}$										
Depth, $\left( \frac{Z}{T} \right)$	Depth, Z (in.)	$A_y$	$y_Q = A_y \left( \frac{Q_g T^3}{EI} \right)$ (in.)	$B_y$	$y_m = B_y \left( \frac{M_g T^2}{EI} \right)$ (in.)	$y = y_Q + y_m$ (in.)	$p_f$ (psi)	$k_i$ (psi)	$k = \frac{1}{\frac{1}{k_i} + \frac{y}{p_f B}}$ (psi)	$n_h = \frac{k}{Z}$ (psi)
0.00	0.0	2.40	0.12	1.60	0.05	0.18	0.0	3,500	0	0.0
0.05	2.2	2.32	0.12	1.52	0.05	0.18	2.0	5,819	175	77.2
0.10	4.5	2.25	0.12	1.45	0.05	0.17	5.7	8,138	490	108.7
0.30	13.5	1.90	0.10	1.10	0.04	0.14	22.3	10,571	2,013	148.9
0.55	24.7	1.55	0.08	0.80	0.02	0.11	31.7	8,183	2,889	116.6
0.90	40.5	1.15	0.06	0.40	0.01	0.07	41.5	6,554	3,724	91.9
1.40	63.0	0.45	0.02	0.10	0.00	0.02	43.1	4,376	3,716	58.9
2.80	126.0	0.10	0.00	0.15	0.00	0.01	96.1	4,881	4,716	37.4
T = relative stiffness factor										
EI = flexural stiffness of pile										
$n_h$ = constant of horizontal subgrade reaction										
B = pile width										
Total $n_h$ = 639.7										
Average $n_h = \frac{\text{Total}}{7.0} = 91.1$										

Table 5. Comparison of Computed Displacements

Load (lb)	Displacement at Groundline (in.)		
	Tabular Solution	Computer Solution	Test Data
10,000	0.18	0.14	0.15
15,000	0.36	0.30	0.28

The realistic handling of the nonlinear soil response is evidenced by the fact that the displacements computed by the tabular method are increased 100% by only a 50% increase in the magnitude of load from 10,000 to 15,000 pounds. Further evidence is given by the resulting magnitudes of  $n_h$  for the two load levels. From Table 4 it can be seen that the computed average values of  $n_h$  for a 10,000-pound load was approximately 91 lb/in.<sup>3</sup> A separate solution (not presented) for a load of 15,000 pounds yielded a value of approximately 58 lb/in.<sup>3</sup>. Therefore, it is shown that the constant of horizontal subgrade reaction,  $n_h$ , of a given soil deposit is not actually a constant.

It is noted that if estimates of other pile response parameters such as slopes, shears, and bending moments are desired, these parameters can be obtained by using the available design charts<sup>17</sup> and the values of  $n_h$  obtained during the displacement computations.

## CONCLUSIONS

From the results of lateral plate bearing tests, lateral load tests on rigid poles, segmental pile tests, lateral load tests on flexible piles, corresponding soil investigations, and theoretical studies of lateral soil pressure-displacement relationships, the following conclusions were reached:

1. For the design of laterally loaded, soil-supported structures, it is necessary to account for the nonlinear response of the soil under loading.

2. Lateral soil pressure-displacement curves can be determined with sufficient ease and accuracy by a representation of these relationships with rectangular hyperbolas of the form

$$\frac{y}{pB} = \frac{1}{k_i} + \frac{1}{p_f} \left( \frac{Z}{B} \right)$$

3. The terms  $k_i$  and  $p_f$  in the above relationship can be defined with sufficient accuracy in terms of the shear strength (undrained for cohesive soils), the depth below the ground surface, and the pile width for both cohesive and noncohesive soils. With noncohesive soils, a knowledge of the effective overburden stress versus depth is required also. Expressions for  $k_i$  and  $p_f$  are presented.

4. These lateral soil pressure-displacement relationships can be utilized in the computer program presented in the Appendix to compute the response of vertical piles to lateral loading. The computer program provides a finite difference solution in an iterative form in order that the nonlinear soil behavior can be considered.

5. For cases where an electronic computer is not available, the tabular solution presented is an expedient means of obtaining solutions to the laterally loaded pile problem while considering the nonlinear soil response.

6. The proposed procedures are applicable for conditions of sustained loading. For cyclic or repetitive loadings, it is concluded that displacements and slopes should be increased by 50% over the computed values and that bending moments, shears, and computed soil pressures should remain unchanged.

## ACKNOWLEDGMENTS

Appreciation is expressed to those personnel who have contributed either directly or indirectly to the securing of the information presented in this report. Included among these contributors were Messrs. J. Drelicharz, H. Loigman, H. Cook, R. Shubeck, and A. Garcia.

## Appendix

### COMPUTER PROGRAM

A format for a once-through solution of Equation 1 has been suggested.<sup>8</sup> This format was followed during this study, but it was not possible to perform a closed, once-through solution because of the nonlinear soil response. Therefore, an iterative procedure was utilized.

The computer code for an iterative finite difference solution of Equation 2 is presented in Table A-1. A similar computer code was presented and discussed in Reference 4, but the code has been changed slightly in order to provide compatibility with the more appropriate procedures for predicting soil response. In addition, other minor refinements have been made, including provisions for considering tapered piles and layered soil systems.

Comment statements are included in the computer code; however, it is desirable to have some additional explanation in order to avoid confusion, especially with regard to the input data. All of the input data are arranged in the same format and each input data card is discussed separately.

#### Card No. 1

- B = pile width at the groundline (in.)
- EI = flexural stiffness of the  
pile at the groundline (lb-in.<sup>2</sup>)
- DX = incremental lengths of the pile  
or pile length divided by 53 (in.)
- PG = groundline shear,  $Q_g$  (lb)
- BMG = bending moment at the groundline,  $M_g$  (in.-lb)

#### Card No. 2

- CEI = variation of EI with depth;  
EIA (value of EI at a depth Z)  
= (CEI) Z + EI (lb-in.)
- T = number of iterations required  
(11 iterations were sufficient in all cases)
- BS = variation of pile width, B, with depth  
for a tapered pile; BA (value of B at a  
depth Z) = (BS) Z + B (in./in.)



Card No. 3

C(1) through C(5) = layer designations with the larger numbers denoting deeper layers; the designations consist of the numeral 1 for clay and 2 for sand

Card No. 4

ZC(1) through ZC(5) = depth to the top of each layer;  
ZC(1) = 0 (in.)

Card No. 5

This card contains coefficients for the computation of the initial subgrade modulus,  $k_i$ , and the lateral bearing capacity,  $p_f$ , of the soil. These coefficients were varied during the study, but a firm set of values has now been proposed as follows:

PFB = 0.25

CK1B = 100

SK1A = 2,000 (psi)

AX = 0.5

Card No. 6

PO1 = effective overburden stress at the ground surface (psi)

PO2 = effective overburden stress at some depth Z2 (psi)

Z2 = depth of a distinct break in the curve of  $\bar{p}_o$  versus Z; usually the depth of the water table (in.)

SL2 = variation of  $\bar{p}_o$  with depth below the depth Z2;

PO (at any depth Z greater than Z2) =  $PO2 + SL2(Z - Z2)$   
(psi/in.)

Each of these parameters should be nonzero in order to avoid having zero denominators; small decimals can be used in place of zeros.

Cards No. 7 and 8

SM(1) through SM(5) = values of vane resistance, S, at the corresponding depths of ZM(1) through ZM(5); again, the values should be nonzero (psi)

SMB = variation of vane resistance with depth below a depth of ZM(5); S [at any depth Z greater than ZM(5)]

= SMB [Z - ZM(5)] + SM(5) (psi/in.)

ZM(1) through ZM(5) = corresponding values of depth,

ZM(1)  $\equiv$  0

A brief explanation of the procedure used for entering vane resistances into the computer solution is in order. As was mentioned previously, the behavior of laterally loaded piles is influenced most extensively by the properties of the soil at shallow depths. In addition, the vane resistance of soil at depths below the surface layers often increases approximately uniformly with depth. Therefore, the typical procedure used in representing S versus Z was to use SM(1) through SM(5) to provide a fairly accurate representation at shallow depths and to use SMB for a less exact average representation at greater depths.

The computer code provides a trial solution for initiation of the iterative solution by using an arbitrary value of k of 300 psi at all points along the length of the pile. With the resulting trial value of displacement at each point and the soil conditions provided, a new value of k is computed for each point. With the revised values of k, the finite difference solution is repeated and new displacements are obtained. This procedure is repeated until convergence is achieved. It was found that satisfactory convergence occurred in all cases with 11 iterations, and the entire solution required less than 2 minutes of time on an IBM 1620 computer.

The accuracy of the computer program was checked in two ways. First, bending moments computed at the ground elevation were compared with magnitudes of bending moment used as input to the solutions. There were negligible differences in the magnitudes, so it was concluded that the counters and index parameters were computed properly. The second method of checking the program consisted of obtaining computer solutions, with k assumed constant with depth and displacement, and then comparing these solutions with results of a theoretical study using an analog computer. Again, the comparison was favorable. It was concluded that the difference-equation method of solution with 53 increments considered along the pile length provided results of sufficient accuracy when realistic soil parameters were considered.

Table A-1. Computer Code

```

      DIMENSION H(111), G(57), Y(59), SM(6), ZM(6), C(6), ZC(6)
C      DATA INPUT
C      PILE WIDTH, PILE STIFFNESS, EFFECTIVE LENGTH DIV. BY 53, GROUNDLINE
C      SHEAR, GROUNDLINE MOMENT.
5  READ 100,B,EI,DX,PG,BMG
C      STIFFNESS VARIATION, ITERATIONS, WIDTH VARIATION.
      READ 100,CEI,T,BS
C      SAND OR CLAY LAYER.
      READ 100,C(1),C(2),C(3),C(4),C(5)
C      DEPTH TO TOP OF LAYER.
      READ 100,ZC(1),ZC(2),ZC(3),ZC(4),ZC(5)
C      SOIL PRESSURE - DEFLECTION CONSTANTS.
      READ 100,PFB,CKIB,SKIA,AX
C      EFFECTIVE OVERBURDEN PRESSURE AND WATER CONDITIONS FOR SAND.
43 READ 100,PO1,PO2,Z2,SL2
C      UNDRAINED SHEAR STRENGTH DATA ( VANE SHEAR ).
33 READ 100,SM(1),SM(2),SM(3),SM(4),SM(5),SMB
C      DEPTHS FOR SHEAR STRENGTH DATA.
      READ 100,ZM(1),ZM(2),ZM(3),ZM(4),ZM(5)
100 FORMAT(5E15.8,F5.2)
      PUNCH 100,B,EI,DX,PG,BMG
      PUNCH 100,CEI,T,BS
      PUNCH 100,C(1),C(2),C(3),C(4),C(5)
      PUNCH 100,ZC(1),ZC(2),ZC(3),ZC(4),ZC(5)
      PUNCH 100,PFB,CKIB,SKIA,AX
      PUNCH 100,PO1,PO2,Z2,SL2
      PUNCH 100,SM(1),SM(2),SM(3),SM(4),SM(5),SMB
      PUNCH 100,ZM(1),ZM(2),ZM(3),ZM(4),ZM(5)
C      ITERATIONS.
      M=T
C      DIFFERENTIAL INCREMENTS.
      N=53
      DX2=DX*DX
      DO 55 L=1,M
      SET=L-1
      N=N+1
      IJ=5
      IK=5
      IF(SET)24,34,24
34 DO 44 J=1,N
      I=J+3
C      INITIATION OF SOIL PARAMETERS.
44 G(I)=300.*DX2*DX2/EI
      GO TO 45
C      START AT TIP OF PILE.
24 DO 56 J=1,N
      I=J+3
      EYE=N-J
      Z=EYE*DX
C      ACTUAL PILE WIDTH.
      BA=BS*Z+B
C      ACTUAL PILE STIFFNESS.
      EIA=CEI*Z+EI
C      SHEAR STRENGTH CALCULATIONS.
      IF(Z-ZM(5))76,86,86
86 S=SMB*(Z-ZM(5))+SM(5)
      GO TO 83
76 IF(Z-ZM(IJ-1))79,89,89
79 IJ=IJ-1
      GO TO 76
89 S=(SM(IJ)-SM(IJ-1))*(Z-ZM(IJ-1))/(ZM(IJ)-ZM(IJ-1))+SM(IJ-1)
83 IF(Z-ZC(IK))87,97,97
87 IK=IK-1
      GO TO 83
C      IS LAYER SAND OR CLAY.

```

Continued

Table A-1. Computer Code (Contd)

```

97 K=ND=C(IK)
GO TO (69,93),KIND
C HYPERBOLIC PARAMETERS FOR CLAY.
69 PF = PFB*S*Z/(B**AX)
CKI = CKIB * S
GO TO 65
C HYPERBOLIC PARAMETERS FOR SAND.
93 IF(Z-Z2)37,37,47
37 PO=PO1+(PO2-PO1)*Z/Z2
GO TO 35
47 PO=PO2+SL2*(Z-Z2)
35 PHI=(25.4-PO/(2.94+0.1225*PO))*S**0.16
HNO=0.664*(10.**((0.038*PHI))+0.049*(10.**((0.034*PHI))*Z/BA
PF=HNO*PO
CKI = SKIA
C RECTANGULAR-HYPERBOLA RELATIONSHIP.
65 YOP=BA/CKI+Y(I)/PF
CNG=DX2*DX2*BA/EIA
56 G(I)=CNG/YOP
C DIFFERENCE - EQUATION SOLUTION.
45 H(4)=2./(2.+G(4))
H(5)=2.*H(4)
H(6)=1./(5.+G(5)-2.*H(5))
H(7)=H(6)*(4.-H(5))
N=N-2
DO 10 I=1,N
J=2*(I+5)-4
K=I+5
H(J)=1./(6.+G(K)-H(J-4)-H(J-1)*(4.-H(J-3)))
10 H(J+1)=H(J)*(4.-H(J-1))
CJ4=2.*DX2*DX2*PG/EI
CJ3=DX2*BMG/EI
N=N+1
K=2*N+4
Y(N)=(CJ4*H(K)*(1.-H(K-2)))
Y(N)=Y(N)-CJ3*H(K)*(2.+2.*H(K-2)-H(K-2)*H(K-3))
Y(N)=Y(N)+CJ3*H(K+1)
A=4.-4.*H(K-1)+4.*H(K-2)-H(K-4)+H(K-1)*H(K-3)
A=A-2.*H(K-2)*H(K-3)+H(K-2)*H(K-4)
Y(N+4)=Y(N)/(1.-H(K-2)-2.*H(K+1)+H(K-1)*H(K+1)+H(K)*A)
Y(N+5)=(CJ3+Y(N+4)*(2.-H(K-1)))/(1.-H(K-2))
Y(N+6)=(H(K+1)*Y(N+5)-Y(N+4))/H(K)
DO 20 J=1,N
I=N-J+4
K=2*I-4
20 Y(I)=-H(K)*Y(I+2)+H(K+1)*Y(I+1)
Y(3)=-Y(5)+2.*Y(4)
Y(2)=Y(6)-2.*Y(5)+2.*Y(3)
SL=(-Y(N+5)+Y(N+3))/(2.*DX)
55 PUNCH 100,Y(N+4),SL
N=N+1
DO 80 J=1,N,2
I=N-J+4
EYE=J-1
Z = EYE * DX
BA = BS * Z + B
EIA = CF1 * Z + F1
BM=EIA*(Y(I+1)-2.*Y(I)+Y(I-1))/DX2
CNG=DX2*DX2*BA/EIA
P=G(I)*Y(I)/CNG
CK=P*BA/Y(I)
C DEPTH, DEFLECTION, MOMENT, SOIL PRESSURE, SUBGRADE MODULUS.
80 PUNCH 100, Z, Y(I), BM, P, CK
GO TO 5
70 PAUSE
END

```

## REFERENCES

1. Naval Civil Engineering Laboratory. Technical Report R-310 Lateral-plate and rigid-pile tests in beach sand, by H.L. Gill. Port Hueneme, Calif., Aug. 1964. (AD 444370).
- 2.—. Technical Note N-670. Lateral plate tests on dry NCEL test sand, by H.L. Gill and T. R. Kretschmer. Port Hueneme, Calif., Nov. 1964. (AD 454265).
- 3.—. Technical Report R-374 Lateral-plate tests with plate diameter varied, by H.L. Gill and T.J. Garcia. Port Hueneme, Calif., Apr. 1965. (AD 613991).
- 4.—. Technical Report R-571. Soil behavior around laterally loaded piles, by H.L. Gill. Port Hueneme, Calif., Apr. 1968. (AD 667833).
- 5.—. Technical Report R-386 Horizontal load tests with a segmental pile, by H.L. Gill and T.R. Kretschmer. Port Hueneme, Calif., July 1965. (AD 617916).
6. M.T. Davisson. Behavior of flexible vertical piles subjected to moment, shear, and axial load, PhD thesis, University of Illinois. Urbana, Ill., 1960.
7. M.T. Davisson and H.L. Gill "Laterally loaded piles in a layered soil system," American Society of Civil Engineers, Proceedings, Journal of the Soil Mechanics and Foundations Division, vol. 89, no. SM3, May 1963, pp. 63-94.
8. H. Matlock and L.C. Reese "Generalized solutions for laterally loaded piles," American Society of Civil Engineers, Proceedings, Journal of the Soil Mechanics and Foundations Division, vol. 86, no. SM5, Oct. 1960, pp. 63-91.
9. Naval Civil Engineering Laboratory. Technical Report R-283 Lateral thrust on piles, by L.W. Heller. Port Hueneme, Calif., June 1964. (AD 601894).
10. L.A. Palmer and P.P. Brown "Analysis of pressure deflection, moment, and shear by the method of difference equations," in Symposium on Lateral Load Tests on Piles, Supplement. Philadelphia, Pa., American Society for Testing Materials, 1955, pp. 22-32. (ASTM Special Technical Publication No. 154-A).

11. R.L. Kondner. "Hyperbolic stress-strain response cohesive soils," American Society of Civil Engineers, Proceedings, Journal of the Soil Mechanics and Foundations Division, vol. 89, no. SM1, Feb. 1963, pp. 115-143.
12. K. Terzaghi. "Evaluation of coefficients of subgrade reaction," Geotechnique, vol. 5, no. 4, Dec. 1955, pp. 297-326.
13. J.B. Hansen "The ultimate resistance of rigid poles against transversal forces," in Danish Geotechnical Institute, Bulletin no. 12. Copenhagen, Denmark, 1961, pp. 5-9.
14. R B. Peck, W E. Hanson, and T.H. Thornburn, Foundation engineering. New York, Wiley, 1953, p. 222.
15. Bureau of Reclamation. Earth manual, a guide to the use of soils as foundations and as construction materials for hydraulic structures. 1st. ed., rev. Denver, Colo., 1963. pp. 51, 314.
16. S. Prakash. Behavior of pile groups subjected to lateral loads, PhD thesis, University of Illinois. Urbana, Ill., 1962.
17. Department of the Navy. Bureau of Yards and Docks. NAVDOCKS DM-7. Design manual: Soil mechanics, foundations and earth structures. Washington, D.C., Feb. 1962.

## LIST OF SYMBOLS

$A_y$	Parameter from design curves	$\bar{p}_0$	Vertical effective stress due to overburden, psi
$B$	Width of pile, in.	$Q$	Horizontal load on pile, lb
$B_y$	Parameter from design curves	$Q_g$	Magnitude of $y$ at ground level, in.
$d$	Horizontal displacement of test segment, in.	$R$	Relative stiffness factor for $k$ constant with depth, in.
$EI$	Flexural stiffness of pile, lb-in <sup>2</sup>	$S$	Vane resistance of soil, psi
$H$	Height of test segment, in.	$T$	Relative stiffness factor for $k$ directly proportional to depth
$h$	Height above ground surface of lateral load on pile, in.	$y$	Horizontal displacement of pile, in.
$k$	Modulus of horizontal subgrade reaction, psi	$y_g$	Magnitude of $y$ at ground level, in.
$k_i$	Value of $k$ at zero displacement, psi	$y_m$	Magnitude of $y$ as a result of a bending moment loading
$k_0$	Value of $k$ assumed constant with depth, psi	$y_Q$	Magnitude of $y$ as a result of a shear loading
$L$	Embedded length of pile, in.	$Z$	Depth below ground level, in.
$L_i$	Liquidity index of soil, %	$\alpha$	Shape factor
$M$	Bending moment in pile, in.-lb	$\theta_g$	Slope of pile at ground level
$M_g$	Applied bending moment at ground level, in.-lb	$\phi$	Angle of internal friction of the sand, degrees
$N$	Standard penetration resistance of soil, blows/ft		
$n_h$	Constant of horizontal subgrade reaction, lb/in. <sup>3</sup>		
$p$	Horizontal soil pressure, psi		
$p_f$	Horizontal bearing capacity of soil, psi		



NAVAL CIVIL ENGINEERING  
LABORATORY  
PORT HUENEME, CALIFORNIA 93041

IN REPLY REFER TO:  
L36/PDT/lg  
YF 38.534.001.01.002  
Serial 1838  
21 September 1970

From: Commanding Officer  
To: Distribution List

Subj: Errata Sheet for Technical Report R-670, "Displacement of Laterally Loaded Structures in Nonlinearly Responsive Soil," by H. L. Gill and K. R. Demars

1. Please make the following pen and ink corrections:

- a. On page 55 instruction number 65 should read— $65 \text{ YOP} = BA/CKI + ABSF(Y(I)/PF)$ .
- b. On page 38, Table 3, Column 10, the equation for k, the absolute value of displacement,  $|y|$ , should be substituted for y.
- c. On pages 40 through 48, Table 4, Column 10, the equation for k, the absolute value of displacement,  $|y|$ , should be substituted for y.

PETER D. TRIEM  
By direction

Reproduced by  
NATIONAL TECHNICAL  
INFORMATION SERVICE  
Springfield, Va. 22151